

# Silencing of cardiac mitochondrial NHE1 prevents mitochondrial permeability transition pore opening

María C. Villa-Abrille,<sup>1</sup> Eugenio Cingolani,<sup>2</sup> Horacio E. Cingolani,<sup>1</sup> and Bernardo V. Alvarez<sup>1</sup>

<sup>1</sup>Centro de Investigaciones Cardiovasculares, Consejo Nacional de Investigaciones Científicas y Técnicas Facultad de Ciencias Médicas, Universidad Nacional de La Plata, La Plata, Argentina; and <sup>2</sup>Heart Institute Cedars-Sinai Medical Center, Los Angeles, California

Submitted 24 August 2010; accepted in final form 28 January 2011

**Villa-Abrille MC, Cingolani E, Cingolani HE, Alvarez BV.** Silencing of cardiac mitochondrial NHE1 prevents mitochondrial permeability transition pore opening. *Am J Physiol Heart Circ Physiol* 300: H1237–H1251, 2011. First published February 4, 2011; doi:10.1152/ajpheart.00840.2010.—Inhibition of Na<sup>+</sup>/H<sup>+</sup> exchanger 1 (NHE1) reduces cardiac ischemia-reperfusion (I/R) injury and also cardiac hypertrophy and failure. Although the mechanisms underlying these NHE1-mediated effects suggest delay of mitochondrial permeability transition pore (MPTP) opening, and reduction of mitochondrial-derived superoxide production, the possibility of NHE1 blockade targeting mitochondria has been incompletely explored. A short-hairpin RNA sequence mediating specific knock down of NHE1 expression was incorporated into a lentiviral vector (shRNA-NHE1) and transduced in the rat myocardium. NHE1 expression of mitochondrial lysates revealed that shRNA-NHE1 transductions reduced mitochondrial NHE1 (mNHE1) by ~60%, supporting the expression of NHE1 in mitochondria membranes. Electron microscopy studies corroborate the presence of NHE1 in heart mitochondria. Immunostaining of rat cardiomyocytes also suggests colocalization of NHE1 with the mitochondrial marker cytochrome *c* oxidase. To examine the functional role of mNHE1, mitochondrial suspensions were exposed to increasing concentrations of CaCl<sub>2</sub> to induce MPTP opening and consequently mitochondrial swelling. shRNA-NHE1 transduction reduced CaCl<sub>2</sub>-induced mitochondrial swelling by 64 ± 4%. Whereas the NHE1 inhibitor HOE-642 (10 μM) decreased mitochondrial Ca<sup>2+</sup>-induced swelling in rats transduced with nonsilencing RNAi (37 ± 6%), no additional HOE-642 effects were detected in mitochondria from rats transduced with shRNA-NHE1. We have characterized the expression and function of NHE1 in rat heart mitochondria. Because mitochondria from rats injected with shRNA-NHE1 present a high threshold for MPTP formation, the beneficial effects of NHE1 inhibition in I/R resulting from mitochondrial targeting should be considered.

ischemia; myocardium; mitochondrial permeability transition pore

SARCOLEMMA Na<sup>+</sup>/H<sup>+</sup> EXCHANGER 1 (NHE1) is a major Na<sup>+</sup> influx pathway that catalyzes the electroneutral exchange of one intracellular H<sup>+</sup> for one extracellular Na<sup>+</sup> across the plasma membrane of cardiac cells. NHE1, which is relatively quiescent under basal conditions, becomes highly active during ischemia in response to intracellular acidosis, leading to NHE1-mediated Na<sup>+</sup> entry in the cell (36). Inhibition of intracellular Na<sup>+</sup> concentration accumulation by increasing Na<sup>+</sup>/H<sup>+</sup> exchange activity and prevention of Ca<sup>2+</sup> overload via Na<sup>+</sup>/Ca<sup>2+</sup> exchanger have been proposed as potential mechanisms of cardioprotection by NHE1 blockade (4).

Address for reprint requests and other correspondence: B. V. Alvarez, Centro de Investigaciones Cardiovasculares, CONICET Facultad de Ciencias Médicas, Universidad Nacional de La Plata, Calle 60 y 120, 1900 La Plata, Argentina (e-mail: balvarez@med.unlp.edu.ar).

Na<sup>+</sup>/H<sup>+</sup> exchanger inhibitors have proven to protect the heart against ischemia-reperfusion (I/R) injury (35). Moreover, the positive effect that NHE1 inhibition exerts on left ventricular systolic function during revascularization therapy after acute myocardial infarction has been documented in a clinical study (49).

NHE1 activity is controlled by intracellular pH and numerous other factors, such as hormones, catecholamines, enzymes, and mechanical stimuli, known to be associated with heart disease. Furthermore, cardiac expression of an activated form of NHE1 that lacks the calmodulin-binding inhibitory domain was sufficient by itself to initiate cardiac hypertrophy and heart failure (44). Constitutively active NHE1 leads to pathological changes in activation of the Ca<sup>2+</sup>-dependent prohypertrophic signaling molecules calcineurin and calmodulin kinase II (44). Similarly, in heart, overexpression of activated NHE1 was recently found to elicit specific pathways of gene activation, inducing an increase in cross-sectional area of cardiomyocyte, interstitial fibrosis, and depressed cardiac function in transgenic mice (58).

The mitochondrial death pathway features the sequential loss of mitochondrial membrane potential (ΔΨ<sub>m</sub>), which is accompanied by irreversible opening of the mitochondrial permeability transition pore (MPTP), release of toxic proteins in the cytoplasm, and activation of proteolytic activity of caspases (54). Recently, a specific NHE1 inhibitor, cariporide, was found to be cardioprotective through its effects on mitochondria (21, 30, 54). The beneficial effect of NHE-1 inhibition by cariporide in hearts subjected to I/R was associated with attenuation of MPTP opening and apoptosis and the resultant mitochondrial dysfunction (30). In addition, Ruiz-Meana and collaborators (48) have shown that inhibition of mitochondrial NHE during ischemia slows both acidification of the mitochondrial matrix and ATP hydrolysis, delaying the progression of ischemic injury and reducing cell death. Whether the beneficial cardiac effects of NHE1 inhibition are secondary to preventing cytosolic Ca<sup>2+</sup> overload or a direct mitochondrial effect needs additional investigation.

The identity of the Na<sup>+</sup>/H<sup>+</sup> exchanger isoform localized in the mitochondria is still controversial. The first Na<sup>+</sup>/H<sup>+</sup> isoform to be identified was NHE1, which has a ubiquitous tissue distribution in mammals (50). Since its discovery, nine other human isoforms have been identified (NHE2–NHE10) (20, 39). While NHE1–NHE6 reside in the plasma membrane or recycling endosomes, NHE7–NHE9 are located within the cell rather than the plasma membrane (20).

Dual distribution of the Na<sup>+</sup>/Ca<sup>2+</sup> exchanger 1–3 (NCX1–3) (25), and Kv1.3 (53), Kir6.2 (22), and Ca<sup>2+</sup>-activated large-conductance (BK) potassium channels (51) at both plasma

membrane and mitochondria, has been documented previously. In addition, connexin 43 (Cx43), a constitutive protein that forms cardiac gap junctions contributing to cell-cell coupling, was also localized in mitochondria (8, 9). Cx43 contains four transmembrane domains as well as amino and carboxy termini located in the cytosol. Cx43 localized in subsarcolemmal mitochondria with its carboxy terminus directed towards the intermembrane space (9). Following this line of thinking, we reason that NHE1 would be involved in the Na<sup>+</sup>/H<sup>+</sup> exchange process in the mitochondria.

To our knowledge, NHE1 function and expression has not been evaluated in cardiac tissues with the assistance of the RNA interference (RNAi) technique. In vivo experiments were performed injecting a lentiviral vector expressing shRNA-NHE1 intramyocardically, with the objective of knocking down the expression of NHE1 in the heart. Transduction of shRNA-NHE1 allowed us to assess the expression and functional role of NHE1 at the subcellular level in the rat heart.

We revealed the expression of NHE1, a typical integral plasma membrane protein, in the heart mitochondria. Furthermore, we demonstrated that inhibition of NHE1 protects heart mitochondria from Ca<sup>2+</sup>-induced mitochondrial swelling and MPTP opening.

## MATERIALS AND METHODS

**Isolation of rat cardiomyocytes.** Adult rats were anesthetized with euthanyl (pentobarbital sodium; 100 mg/kg ip). The hearts were rapidly removed, and ventricular myocytes were obtained by enzymatic dissociation using standard protocols (2). Animal protocols were reviewed and approved by the Animal Welfare Committee of La Plata School of Medicine and performed in accordance with the *Guide for the Care and Use of Laboratory Animals*, published by the National Institutes of Health, and the Argentine Republic Law No. 14346 concerning animal protection. The hearts were rapidly removed, and ventricular myocytes were obtained by enzymatic dissociation, using standard protocols (2).

**Isolation of rat heart membranes.** Rat heart membranes were prepared from freshly isolated left ventricles, which were separated and homogenized with a Brinkmann Homogenizer (Brinkmann Instruments, Westbury, NY) in 4 ml of ice-cold solution containing 0.32 M sucrose, 1 mM EGTA, 0.1 mM EDTA, 10 mM HEPES, pH 7.5, and protease inhibitors (MiniComplete tablets; Roche). Homogenates were centrifuged at 1,440 g for 5 min in a Beckman G5–6K centrifuge. Supernatants were removed and centrifuged at 66,700 g for 30 min at 4°C in a Beckman TLA 100.4 rotor. The resulting membrane fraction was resuspended in 300 µl of PBS containing (in mM): 140 NaCl, 3 KCl, 6.5 Na<sub>2</sub>HPO<sub>4</sub>, and 1.5 KH<sub>2</sub>PO<sub>4</sub>, pH 7.5. The Quant-iT protein assay kit (Molecular Probes/Invitrogen Labeling and Detection, Eugene, OR) was used to determine protein concentration on a Qubit fluorometer (Invitrogen) according to the manufacturer's instructions, and 100 µg of protein were used for immunoblots.

**Isolation of rat heart mitochondria.** Rat heart mitochondria were isolated by differential centrifugation, according to a modified method described previously (38). Briefly, hearts were rapidly excised from pentobarbital-anesthetized rats and placed in an ice-cold isolation buffer (IB) containing (in mM): 75 sucrose, 225 mannitol, and 0.01 EGTA, pH 7.4. After both atria and right ventricle were removed, the remaining left ventricle was homogenized manually with a Dounce homogenizer (~20 strokes) in the presence of proteinase (0.8 mg in 5 ml of IB, P8038; Sigma). Homogenized tissue was centrifuged 5 min at 480 g (4°C), and the pellet containing unbroken cells and nuclei was discarded. The resulting supernatant containing the mitochondrial fraction was further centrifuged at 7,700 g (3 × 5 min), and the final pellet was resuspended in IB with no EGTA and further centrifuged at

7,700 g for 5 min. Protein concentration of the mitochondrial suspension was determined as described above.

**Isolation of Percoll-purified mitochondria.** To isolate purified mitochondria, rat heart ventricles were homogenized with a Polytron in *sucrose buffer H* containing (in mM): 250 sucrose, 10 HEPES-KOH, 1 EDTA, and 1 dithiothreitol, pH 7.40, with protease inhibitors (MiniComplete tablets; Roche). The homogenate was centrifuged for 5 min at 2,000 g at 4°C to remove cell debris and nuclei. Postnuclear homogenate was centrifuged for 10 min at 10,000 g, and the resulting pellet was further resuspended in 1 ml of *buffer H* and homogenized in a Dounce homogenizer to obtain the crude mitochondria. Briefly, 1 ml of the crude mitochondria suspension was loaded in a tube containing 9 ml of 30% (vol/vol) Percoll in *buffer H* and centrifuged for 30 min at 95,000 g in a 70.1 Ti rotor, in a Beckman LE-80K ultracentrifuge. After centrifugation, the tubes contained two distinct bands separated by a clear zone. The lower brownish band was collected and diluted fourfold in cooled *buffer H*. To remove the Percoll, the samples were centrifuged for 10 min at 6,300 g, and the pellet was washed two times with cold *buffer H* to obtain pure mitochondria. The whitish upper layers of the self-forming Percoll gradient were collected and diluted fourfold in cold *buffer H*. They were centrifuged at 10,000 g for 10 min, and the resulting pellet was washed two times with cold *buffer H* to obtain the mitochondrial-associated vesicle fraction. The supernatant of this centrifugation was centrifuged at 100,000 g for 1 h to obtain the membrane-associated mitochondrial (MAM) fraction.

**Mitochondrial swelling determination.** Mitochondrial swelling was measured as a decrease in the 90° light-scattering signal induced by the addition of either 50 µM CaCl<sub>2</sub> or 200 µM CaCl<sub>2</sub>, which promotes the influx of solutes through the opened MPTP and decreases light scattering. After 5 min of preincubation at 37°C in a medium containing (in mmol/l) 120 KCl, 20 MOPS, 10 Tris-HCl, and 5 KH<sub>2</sub>PO<sub>4</sub>, pH 7.4, 50 µM or 200 µM CaCl<sub>2</sub> were added to induce MPTP opening (6, 40). The decrease in light scattering was detected with a temperature-controlled Aminco Bowman Series 2 spectrofluorometer operating with continuous stirring at excitation and emission wavelengths of 520 nm. Light-scattering decrease was calculated for each sample as the difference between the values before and after the addition of CaCl<sub>2</sub>. The experiments were performed in the absence and in the presence of the NHE1 inhibitor cariporide (10 µM). The effect of the inhibitors was expressed as the percentage of decrease in light scattering compared with that induced by 200 µM CaCl<sub>2</sub>.

**Double immunostaining of rat cardiac myocytes and human embryonic kidney 293 cells, and analysis by confocal microscopy.** Freshly isolated adult rat cardiomyocytes were fixed on 22 × 22-mm laminin (30 µg/ml)-coated glass cover slips, or human embryonic kidney (HEK) 293 cells were fixed on poly-L-lysine (10 µg/ml)-coated glass cover slips, and incubated at 37°C for 30 min to allow attachment. Cells were rinsed with PBS and fixed in 4% (wt/vol) paraformaldehyde for 15 min at room temperature (myocytes, HEK 293 cells), followed by methanol fixation-permeabilization [myocytes, ice-cold 100% (vol/vol) methanol, 5 min at –20°C]. Myocytes were then washed with PBS and permeabilized with 0.1% Triton X-100 (vol/vol) in PBS for 15 min at room temperature, and HEK 293 cells were washed with PBS and permeabilized with 0.1% Triton X-100 (vol/vol) in PBS for 2 min at room temperature. After washing (2 × 5 min with PBS) and blocking (5% BSA in PBS, 20 min) were completed, myocytes or HEK 293 cells were incubated with a combination of primary rabbit polyclonal anti-NHE1 antibody (sc-28758, 1:500; Santa Cruz) and mouse anti-cytochrome *c* oxidase complex I (COXI) antibody (sc-58347, 1:2,000; Santa Cruz) (1:100 dilutions), followed by secondary chicken anti-rabbit conjugated to Alexa fluor 488 and chicken anti-mouse conjugated to Alexa fluor 594 (1:100 dilutions). Immunostained cells were mounted in Prolong anti-fade solution (Molecular Probes) and imaged with an Olympus Bx51

laser-scanning confocal microscope (myocytes) or a Zeiss LSM-410 laser-scanning confocal microscope (HEK 293 cells). Images were collected with an oil immersion  $\times 60$  objective, confocal aperture 0.2, zoom  $\times 1.5$  (numerical aperture 1.4, plan Apochromat) at a resolution of 0.5- to 0.7- $\mu\text{m}$  field depth. Filtering was used to integrate the signal collected over four frames to decrease noise, with a frame size of  $1,024 \times 1,024$  (myocytes, scan time of 3.2 s/frame) or a frame size of  $520 \times 520$  (HEK 293 cells). Images were saved and visualized with the Fluoview 3.3 Software (myocytes) or the LSM Image Browser (HEK 293 cells).

**Colocalization analysis.** For the colocalization assay of isolated rat cardiomyocytes, images were obtained with the same settings of the confocal microscope, except for detector gain adjustments in the green channel that were performed to normalize saturation levels. Images were analyzed using the colocalization menu of the Image-Pro Plus software. Regions of interest (ROIs) covering the entire area of the cardiomyocyte were created, followed by the adjustment of the red channel lower threshold to exclude background staining from further analysis. The colocalization statistics were determined from the points included within ROIs and presented as Pearson's correlation values that can vary between zero and one. Pearson's correlation reflects the linear relationship between two variables. A correlation of zero means that there is no linear relationship between the variables, whereas a correlation of one indicates a perfect positive linear relationship.

**Protein expression.** Expression constructs for human hemagglutinin (HA) epitope-tagged NHE1-HA or rat AE3-HA (AE3fl) have been described previously (2). HEK 293 cells were individually transfected with NHE1-HA or AE3-HA cDNAs using Lipofectamine 2000 reagent. Cells were grown at 37°C in an air-CO<sub>2</sub> (19:1) environment in DMEM medium supplemented with 5% (vol/vol) FBS and 5% (vol/vol) calf serum.

**Isolation of HEK 293 cell mitochondria.** Mitochondria-enriched fractions from HEK 293 cells were prepared for immunoblot analysis of NHE1-HA and AE3-HA expression in transfected cells. Cells grown in 100-cm<sup>2</sup> plates (Corning) to  $\sim 80\%$  confluence at 37°C and 5% CO<sub>2</sub> were trypsinized and sedimented by centrifugation. The cell pellet was washed in ice-cold PBS and then resuspended in 400  $\mu\text{l}$  of ice-cold STEI buffer (in mM: 0.25 sucrose, 10 Tris base, pH 7.2, 2 EDTA, and 0.1 phenylmethylsulfonyl fluoride). Cells were homogenized by 30 strokes in a tight-fitting homogenizer followed by centrifugation at 700  $g$  for 10 min at 4°C. The supernatants containing mitochondria were then sedimented at 11,000  $g$  for 10 min at 4°C two times to isolate the cytosolic fraction, whereas the pellet was resuspended in 200  $\mu\text{l}$  of STEI, centrifuged again as above, and then resuspended in 100  $\mu\text{l}$  of IPB buffer. Finally, the extracts from the mitochondrial-enriched fractions were prepared by addition of 2 $\times$  SDS-sample buffer and subjected to SDS-PAGE.

**Immunodetection.** Cell samples (50  $\mu\text{g}$  protein), heart lysates (50  $\mu\text{g}$  protein), heart mitochondrial lysates (50  $\mu\text{g}$  protein for lysates and 100  $\mu\text{g}$  protein for immunoprecipitates), HEK 293 mitochondria lysates, or Percoll-purified mitochondria were resolved by SDS-PAGE on 8–10% acrylamide gels, as indicated. Proteins were transferred to polyvinylidene fluoride membranes and then incubated with rabbit anti-NHE1, mouse anti-NHE1 (MAB3140, 1:2,000; Chemicon), goat anti-NHE1 (sc-16097, 1:1,000; Santa Cruz), rabbit anti-Na<sup>+</sup>-K<sup>+</sup>-ATPase (sc-28800, 1:1,000; Santa Cruz), goat anti-transferin receptor [TR (CD71), sc-7087, 1:1,000; Santa Cruz], mouse anti-COXI, mouse anti-GAPDH (sc-47724, 1:2,000; Santa Cruz), mouse anti- $\beta$ -actin (sc-47778, 1:1,000; Santa Cruz), or mouse anti-HA (16B12, 1:2,000; Covance). Immunoblots were then incubated with 1:1,000 dilution of donkey anti-rabbit IgG (sc-2317; Santa Cruz), mouse anti-goat IgG (sc-2354; Santa Cruz), or sheep anti-mouse IgG (NA931V; Amersham Biosciences) conjugated to horseradish peroxidase. Blots were visualized with enhanced chemiluminescence reagent (ECL; Millipore) and a Chemidoc Station (Bio-Rad) and quantified using ImageJ analysis software.

**Immunoprecipitation.** Homogenates of rat ventricles were centrifuged at 1,440  $g$  for 5 min in a Beckman G5–6K centrifuge. Supernatants (4 ml corresponding to a total of  $\sim 2$  mg of protein of heart lysates) were removed and applied to 50  $\mu\text{l}$  protein A-Sepharose (50% slurry) for 3 h at 4°C. After centrifugation (5 min, 8,000  $g$ ), lysates were incubated overnight with rabbit polyclonal anti-NHE1 antibody (6  $\mu\text{l}$ , 1.2  $\mu\text{g}$  IgG) or nonimmune rabbit serum (6  $\mu\text{l}$ ). Resin was washed consecutively with wash 1 (0.1% Igepal, 1 mM EDTA, 0.15 M NaCl, and 10 mM Tris-HCl, pH 7.5), wash 2 (2 mM EDTA, 0.05% SDS, and 10 mM Tris-HCl, pH 7.5), and wash 3 (2 mM EDTA and 10 mM Tris-HCl, pH 7.5). After centrifugation (2,000  $g$ ), resin was resuspended in an equal volume of 2 $\times$  SDS-PAGE sample buffer. Samples were electrophoresed on 8% acrylamide gels. Immunoblots were probed with rabbit anti-NHE1 antibody (1:1,000 dilutions) or goat anti-NHE1 antibody (1:1,000 dilutions).

**Tissue preparation, postembedding immunohistochemistry, and electron microscopy analysis.** Rat papillary muscles excised from left ventricles were harvested in 0.1 M phosphate buffer (PBS, pH 7.4) and fixed for 2 h with 2% glutaraldehyde at 4°C. Also, isolated heart mitochondria were fixed for 2 h in 2% glutaraldehyde fixative. After fixation, the cells and tissue blocks were rinsed with PBS and postfixed with 1% osmium tetroxide (2 h, 4°C). Tissues were then dehydrated, infiltrated, and included in Epoxy resin for 36 h subsequently at 35, 45, and 60°C to allow polymerization. Ultrathin sections (60 nm thick) were cut with a Reichert-J Super Nova microtome and collected on copper grids. After being washed with PBS containing 0.2% gelatin (PBSG), papillary muscle sections included on copper grids were permeabilized with 0.5% Triton X-100 in PBSG for 15 min at room temperature. Sections were blocked with 5% BSA in PBSG for 15 min at room temperature and labeled with the rabbit anti-NHE1 IgG antibody in PBSG (1:50 dilution, 14–16 h at 4°C). After being washed with PBSG buffer, samples were incubated with protein A conjugated to 14-nm gold particles (1:20 dilution) in PBSG. As controls, the primary antibody was omitted. After immunohistochemistry, samples were finally contrasted with lead citrate (1%) and uranyl acetate (1%) and viewed with a JEOL JEM 1200-EXII Electron Microscope. Micrograph images were captured and collected with an Erlangshen ES 1000 W digital camera.

**Construction and production of lentiviral vectors.** A third-generation lentiviral vector capable of expressing a reporter gene under the CMV promoter and shRNA under the RNA polymerase III H1 promoter was produced as previously described (14). Briefly, the NHE1 shRNA was subcloned into a third-generation lentiviral vector plasmid that expresses DsRed under the CMV promoter and shRNA under the RNA polymerase III H1 promoter (PPT.C.DsRed.H1). The shNHE1 short-hairpin RNAi sequence was constructed inserting 5'-GATAGGTTTCCATGTGATC-3' (positive strand), followed by: 5'-GTTCTTCAAGAGAGAAC-3' (loop), 5'-ATCACATGGAAACCTATC-3' (negative strand), and 5'-ATCACATGGAAACCTATC-3' (terminator) at the BamHI cloning site (5') and PacI cloning site (3'), following the H1 RNA Polymerase promoter, to generate PPT.C.DsRed.H1.shNHE1. The shSCR short-hairpin RNAi sequence was constructed inserting a noncoding, disorganized nucleotide sequence at the cloning site. For viral vector production, HEK 293T cells were plated in T75-cm<sup>2</sup> flasks to obtain 80–90% confluency on the day of transfection, and cotransfected with a four-plasmid vector system, using Lipofectamine 2000 (Invitrogen). The crude viral suspension was harvested from 293T cell cultures 48 and 72 h after transfection, filtered (0.2  $\mu\text{m}$ ), and concentrated using Centricon Plus-70 filter columns (100,000 molecular weight cut-off; Millipore) at 70,000  $g$  (2 h, 8°C) (7). Vector aliquots were subsequently stored at  $-80^\circ\text{C}$  until use. Vector titers were determined measuring fluorescence of positive HEK 293 cells, transduced with serial viral dilutions in 293T cells, in the presence of 10  $\mu\text{g}/\text{ml}$  of polybrene (Sigma).

**Injection of lentiviral vector and transduction efficiency analysis.** We elected to deliver a small-hairpin RNA (shRNA) targeting rat heart NHE1 (shRNA-NHE1) to downregulate the expression of

mNHE1. This sequence, which was proven effective in reducing whole NHE1 protein expression in cultured fibroblasts, was used here (1). Four- to five-month-old male Wistar rats underwent left thoracotomy in the fourth or fifth intercostal space under general anesthesia, isoflurane inhalation, 4% for induction and 2.5% for maintenance, used in a gas mixture with oxygen and delivered through ventilation by using a positive-pressure respirator (model 680; Harvard, South Natick, MA). The heart was exposed, and the PPT.C.DsRed.H1.shNHE1 lentivirus ( $\sim 2 \times 10^7$  transducing units in 200  $\mu$ l volume, multiplicity of infection  $\sim 80$ ) was injected at two sites in the anterolateral wall of the left ventricle using a 30-gauge needle ( $n = 4$ ) (7). As a control, normal rats were injected with 200  $\mu$ l of saline solution (sham) at the left ventricle ( $n = 5$ ). After injection, the lungs were inflated by increasing positive end-expiratory pressure, and the thoracotomy site was closed in layers. Immediately after surgery, rats were returned to their cages and carried to a recovery room of our faculty animal facility until death (2 wk or 1 mo later). Rats had ad libitum access to food and water. Two weeks after injections, hearts were removed, and mitochondria were prepared from left ventricles as described in previous sections. To evaluate transduction efficiency, isolated cardiomyocytes from injected animals were fixed to 30  $\mu$ g/ $\mu$ l laminin-coated glass cover slips, mounted on glass slides, and evaluated by fluorescence microscopy for DsRed fluorescence.

**Statistical analysis.** All results are presented as means  $\pm$  SE. Significance of differences between any two groups was determined by the Student's *t*-test or ANOVA. A final value of  $P < 0.05$  was considered significant for all analyses. All probability values reported are two-sided.

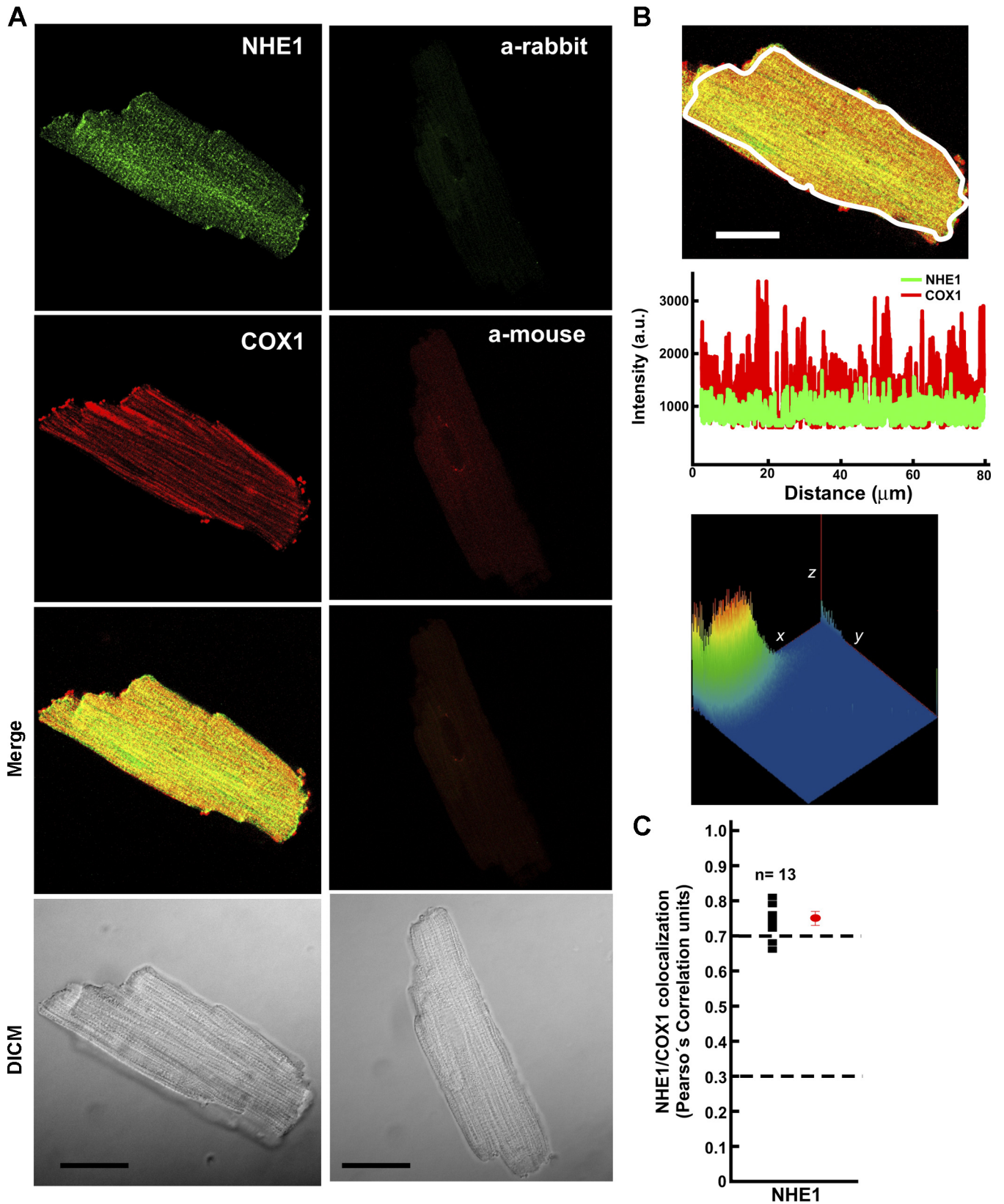
## RESULTS

**Distribution of the NHE1 Na<sup>+</sup>/H<sup>+</sup> exchanger in isolated cardiomyocytes.** To determine the cellular location of NHE1 in the intact rat myocardium, we used confocal immunofluorescence microscopy analysis of isolated adult rat cardiomyocytes, using an isoform-specific rabbit polyclonal anti-NHE1 antibody that recognizes human NHE1. Rat NHE1 has a high degree of sequence similarity with human NHE1 and was therefore anticipated to react with the anti-human NHE1 antibody. NHE1 protein expression was localized predominantly to the intercalated discs regions, with less prominent labeling of transverse tubules (Fig. 1A, left), as shown in previous reports (52). Within the cell, a longitudinal punctuate labeling of NHE1, reminiscent of organelles such as mitochondria, was observed. Therefore, we performed double-labeling experiments of rat cardiomyocytes using anti-COXI antibody, a mitochondrial protein, and anti-NHE1 antibody. NHE1 colocalized with COXI to some extent (merged images), suggesting expression of NHE1 in mitochondria (Fig. 1A, left). No fluorescent signal was detected in cardiomyocytes treated with secondary antibodies alone (Fig. 1A, right). Quantification analysis was performed in isolated cardiomyocytes double-labeled with anti-NHE1 and anti-COXI antibodies. Line scans

of the images show a certain degree of overlapping between NHE1 (green) and COXI (red), also observed in a three-dimensional image view, suggesting colocalization of both proteins (Fig. 1B). The quantification of the colocalization of green channel pixels (NHE1) with red channel pixels (COXI) was performed using the "colocalization" function of the image analysis software Image-Pro Plus. The association degree of NHE1 with the mitochondrial inner membrane marker COXI is depicted as a Pearson's correlation coefficient (*r*) (Fig. 1C) where the *r* values between  $-0.3 \pm 0.3$  indicate little or no association,  $+0.3 \pm 0.7$  weak positive association, and  $+0.7 \pm 1.0$  strong positive association. Using this analysis, we found that NHE1 shows a high degree of colocalization with COXI ( $r = 0.75 \pm 0.01$ ,  $n = 13$ ; see Fig. 4B), suggesting the localization of NHE1 to the subcellular mitochondria of the rat myocardium.

**Expression of the NHE1 Na<sup>+</sup>/H<sup>+</sup> exchanger in rat heart mitochondria.** To determine the role of the NHE1 in the heart mitochondria, we examined the expression of NHE1 in deenergized mitochondria isolated from normal adult rat left ventricular myocardium. The purity of mitochondrial fractions obtained from rat heart was assessed by electron microscopy (EM). Electron micrographs showed well-preserved elliptical-shaped mitochondria with intact inner and external mitochondrial membranes (Fig. 2A). Expression of NHE1 protein was studied in purified rat heart mitochondria lysates by immunoprecipitation. NHE1 was immunoprecipitated using rabbit anti-NHE1 antibodies, and corresponding immunoblots were probed with either rabbit anti-NHE1 antibody (Fig. 2B) or goat anti-NHE1 antibody (Fig. 2C). Both antibodies recognized NHE1 in mitochondrial lysates and immunoprecipitates, and NHE1 expression analysis (AU/ $\mu$ g protein,  $n = 3$ ) was performed (Fig. 2D). Importantly, nonimmune rabbit serum failed to immunoprecipitate NHE1 from mitochondrial lysates (Fig. 2, B and C). To verify these results, cardiac mitochondrial lysates were analyzed together with HEK 293 lysates, which endogenously express low levels of the NHE1 protein. Both lysates were electrophoresed, and corresponding immunoblots were probed with mouse monoclonal anti-NHE1 antibody (Fig. 3A). Immunoblots revealed bands with the same electrophoretic mobility for both lysates. Mitochondrial preparations may contain some membrane contaminants that could affect previous conclusions. To exclude this possibility, markers of the plasma membrane (Na<sup>+</sup>-K<sup>+</sup>-ATPase), cellular recycling endosomal compartment (TfR), or mitochondria (COXI) were blotted and probed with specific antibodies. HEK cultured whole cell lysates, used as positive controls, expressed Na<sup>+</sup>-K<sup>+</sup>-ATPase (A), TfR (B), and COXI (C) proteins, to some extent. Immunoblots shown on Fig. 3, B-D, confirmed that the mito-

Fig. 1. Expression of Na<sup>+</sup>/H<sup>+</sup> exchanger 1 (NHE1) in rat isolated cardiomyocytes. A: double-labeling images of adult mouse cardiomyocytes ( $\times 1.5$  zoom). Freshly isolated adult mouse cardiomyocytes were double stained with rabbit anti-NHE1 antibody or with goat anti-cytochrome *c* oxidase complex I (COXI) antibody as indicated (right) and in green and red staining, respectively, followed by Alexa fluor 488-conjugated chicken anti-rabbit IgG and Alexa fluor 596-conjugated chicken anti-mouse IgG. Colocalization of NHE1 and COX is indicated as a merged image and with yellow staining. Cardiomyocytes labeled with secondary antibodies only are indicated in the images (right). Images were collected with an Olympus Bx61 laser-scanning confocal microscope. Bars = 20  $\mu$ m. DICM, differential interference contrast microscopy. B: histogram showing cell frequency based on the fluorescence intensity of both green and red channel signal corresponding to the entire cardiomyocyte merge image at higher magnification ( $\times 2.5$  zoom). Line scans indicate colocalization between NHE1 (green) and COXI (red) and correlate to the white line drawn on top. Bottom: three-dimensional imaging view of color colocalization. Bar = 20  $\mu$ m. C: the colocalization degree of NHE1 with COXI protein was performed using the image analysis software Image Pro Plus. The values shown in C represent Pearson's correlation units (*r*) that reveal the degree of association of pixels in different channels of the confocal image ( $n$ , no. of cells analyzed).



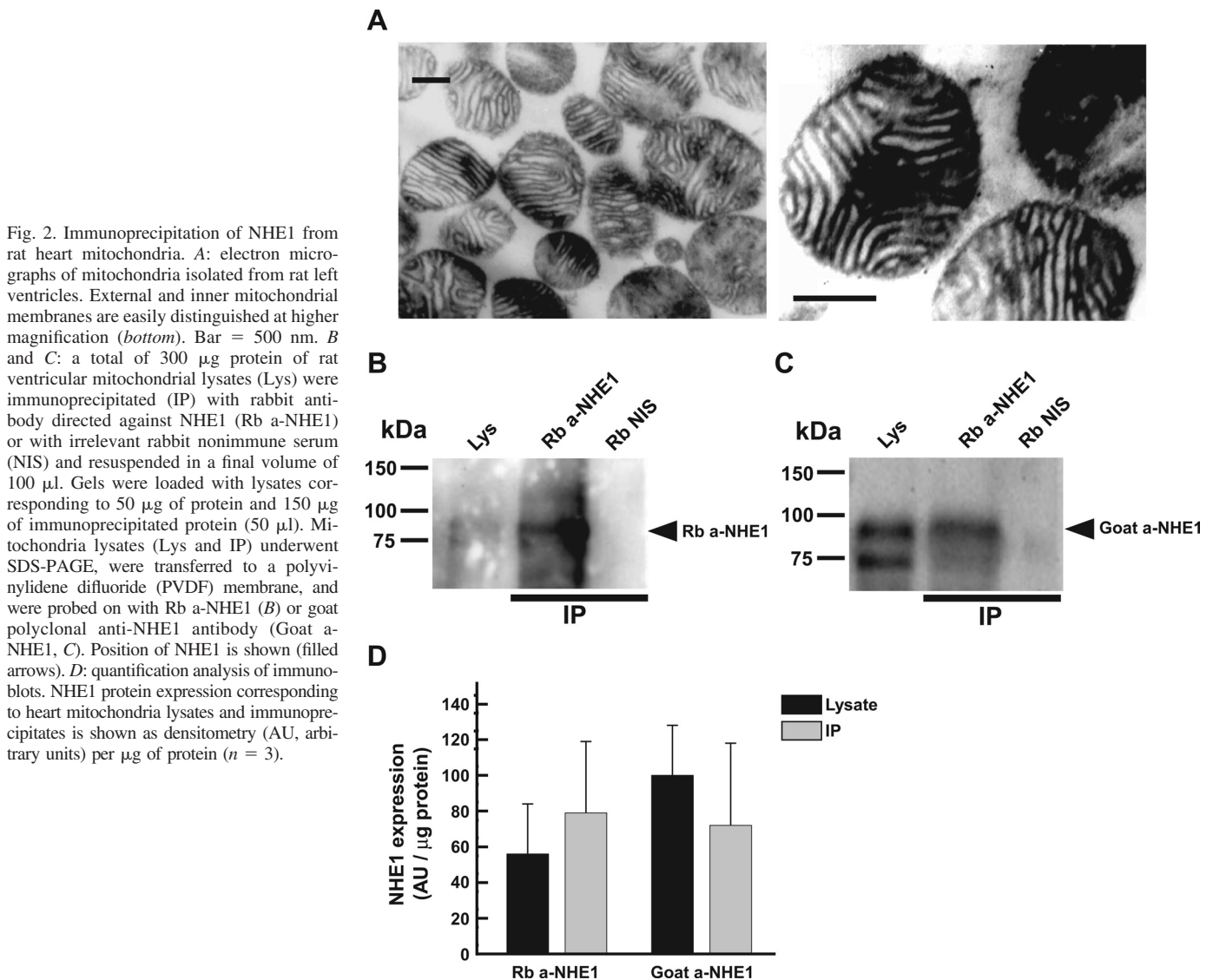


Fig. 2. Immunoprecipitation of NHE1 from rat heart mitochondria. *A*: electron micrographs of mitochondria isolated from rat left ventricles. External and inner mitochondrial membranes are easily distinguished at higher magnification (*bottom*). Bar = 500 nm. *B* and *C*: a total of 300  $\mu$ g protein of rat ventricular mitochondrial lysates (Lys) were immunoprecipitated (IP) with rabbit antibody directed against NHE1 (Rb a-NHE1) or with irrelevant rabbit nonimmune serum (NIS) and resuspended in a final volume of 100  $\mu$ l. Gels were loaded with lysates corresponding to 50  $\mu$ g of protein and 150  $\mu$ g of immunoprecipitated protein (50  $\mu$ l). Mitochondria lysates (Lys and IP) underwent SDS-PAGE, were transferred to a polyvinylidene difluoride (PVDF) membrane, and were probed on with Rb a-NHE1 (*B*) or goat polyclonal anti-NHE1 antibody (Goat a-NHE1, *C*). Position of NHE1 is shown (filled arrows). *D*: quantification analysis of immunoblots. NHE1 protein expression corresponding to heart mitochondria lysates and immunoprecipitates is shown as densitometry (AU, arbitrary units) per  $\mu$ g of protein ( $n = 3$ ).

chondrial lysates used for immunoprecipitation and immunoblotting experiments were enriched in mitochondria, without other major cellular contaminants. A small but detectable fraction of dense endosomes containing TfR was observed in the heart mitochondrial preparation (Fig. 3*B*).

All NHE1 antibodies used herein are specific antibodies directed against the COOH-terminal domain of NHE1. Whereas the mouse anti-NHE1 antibody targets the entire (~300 amino acids) COOH terminus of NHE1, rabbit anti-NHE1 and goat anti-NHE1 recognizes the last 160 amino acid and last 20 amino acid epitopes of the NHE1 cytoplasmic COOH-terminal tail, respectively, targeting NHE1 and not other NHE isoforms (Fig. 4).

In additional experiments, we examined the expression of NHE1 in Percoll-purified mitochondria on immunoblots. Expression of NHE1 was observed in crude and pure mitochondrial lysates but not in MAM lysates (Fig. 5*A*).

To determine if NHE1 is targeted to mitochondria as predicted, dual-labeling experiments were carried out in HEK 293 cells, which express endogenous NHE1, using a mitochondrion-specific marker, COXI, and specific anti-NHE1 antibody. As

demonstrated in a cluster of HEK cells (Fig. 5*B*), the red fluorescence from the COXI was found primarily in clusters of punctuate extranuclear sites, consistent with mitochondrial localization. The green signal emitted by NHE1 protein accumulates in the surface of the cell and as a punctuate labeling in different subregions of the cell. Colocalization of signals from COXI and NHE1 is indicated in yellow/orange when the red and green scans are overlaid (Fig. 5*B*). This pattern represents the staining seen in all experiments. These data suggest that, in addition to plasma membrane localization, NHE1 is most likely targeted to the mitochondria of HEK 293 cells.

The subcellular distribution of NHE1 was also studied in HEK 293 cells individually transiently transfected with NHE1-HA or a HA-epitope tag AE3 anion exchanger cDNA. Mitochondria were isolated from HEK 293 cells transfected with NHE1-HA or AE3-HA, and mitochondrial lysates were resolved by SDS-PAGE, blotted, and probed with anti-HA antibody, or anti-COXI antibody (Fig. 5*C*). HEK 293 mitochondria expressed NHE1-HA, which extends the finding of subcellular NHE1 expression to other cell types. However, AE3, a protein localized in sarcolemma, T tubules, and sarco-

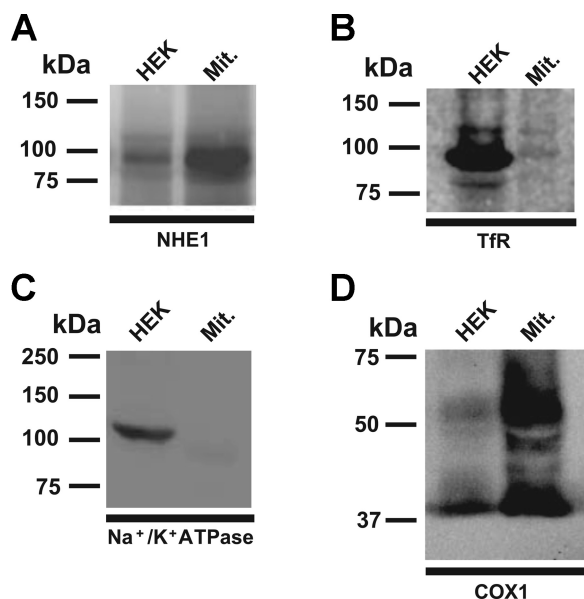


Fig. 3. Expression of NHE1 Na<sup>+</sup>/H<sup>+</sup> exchanger, Na<sup>+</sup>-K<sup>+</sup>-ATPase, transferrin receptor (TfR), and COXI in HEK cells and heart mitochondria (Mit). HEK 293 cell whole lysate samples (50  $\mu$ g) and rat heart mitochondrial lysates (100  $\mu$ g) were analyzed by 7.5% SDS-PAGE (A-C) or 10% SDS-PAGE (D), transferred to PVDF membranes, and probed with antibodies indicated at the bottom of each blot directed against NHE1, Na<sup>+</sup>-K<sup>+</sup>-ATPase, TfR, or COXI.

plasmic reticulum of cardiomyocytes (3), and predominantly at the cell surface of HEK 293-transfected cells (13), was not found in mitochondrial lysates. Colocalization signals of NHE1-HA-transfected or AE3-HA-transfected HEK 293 cells with endogenous COXI were quantified with the Image-Pro Plus software (data not shown). NHE1-HA showed a strong positive association degree with COXI ( $r = 0.70 \pm 0.07$ ,  $n = 4$ ), whereas AE3-HA was weakly associated with COXI ( $r = 0.31 \pm 0.06$ ,  $n = 5$ ), demonstrating again localization of NHE1-HA to the subcellular mitochondria of the HEK cells.

Taken together, these experiments demonstrate the expression of the NHE1 protein in mitochondria isolated from rat ventricular myocardium and mitochondria isolated from HEK 293 cells transfected with NHE1-HA cDNA.

Proteins localized in mitochondria have a mitochondrial localization signal in their NH<sub>2</sub> terminus. The mitochondrial localization prediction program, MITOPROT Software, was used to evaluate the probabilities of NHE1 mitochondrial localization. The amino acid sequences for the human NHE family members, human COXI, and human Na<sup>+</sup>-K<sup>+</sup>-ATPase  $\alpha_2$ -subunit were retrieved from the Swiss Prot database and analyzed by MITOPROT (Table 1). There is a strong prediction for mitochondrial localization of NHE1 (86%), and NHE6 (99%), and to a lesser extent for NHE3 (59%), but not the other NHE isoforms. Indeed, the mitochondrial localization probability for NHE1 and NHE6 was similar to that of the human mitochondrial protein COXI (98%). NHE6 has been recently identified in early/recycling endosomes and stereocilia of sensory hair cells (10, 29). Consistent with its plasma membrane localization, Na<sup>+</sup>-K<sup>+</sup>-ATPase  $\alpha_2$ -subunit has a low mitochondrial localization prediction (32%). Interestingly, all vertebrates share high prediction of NHE1/nhe1 localization to mitochondria, ranging from 0.46 (birds, lowest) to 0.96 (fish,

highest), and from 0.53 (pig, lowest) to 0.89 (rabbit, highest) among mammals (Table 2).

**Subcellular localization of NHE1 and COXI in the myocardium.** There is no evidence, to our knowledge, of high-resolution immunogold analysis of any NHE isoform localized to the mitochondria. Herein, we explored the subcellular localization of NHE1 and COXI in rat left ventricular papillary muscle sections studied in detail, using immunogold EM. The advantage this method provides is that it examines at a very high resolution the location of the protein in the ultrastructure, as it exists in a normal cell or tissue. For this purpose, rat papillary muscle sections were probed with rabbit anti-NHE1 antibody, or mouse anti-COXI antibody, followed by detection with protein A conjugated to 14-nm gold particles. A total of 12 grids were analyzed for each protein. In the heart sections, labeling of NHE1 was clearly observed in mitochondria, at low- and high-power magnifications (Fig. 6, A, B, and E). Gold particles were quantified, and an average of  $3.46 \pm 1.12$  particles were observed (20 grids, 10 mitochondria/grid). Mitochondria presented a minimum of 1 particle and a maximum of 25 particles, corresponding to NHE1 expression. Labeling of COXI was also observed in the mitochondria (Fig. 6, C and F), whereas muscle sections treated only with protein A gold conjugated did not display any gold particles and were therefore immunonegative (Fig. 6D). The localization of immunogold particles suggests the existence of both NHE1 and COXI in the rat heart mitochondria.

Cardiomyocytes contain subsarcolemmal (SSM) and interfibrillar (IFM) mitochondria, which differ in their respiratory and Ca<sup>2+</sup> retention capacity. In our immunogold analysis of NHE1 expression in cardiac muscle mitochondria, we clearly identified NHE1 in IFM (Fig. 6, A and B). We could not, however, exclude the expression of NHE1 in the SSM population of cardiomyocytes.

We conclude that NHE1 is present in the myocardium and located in cardiomyocyte mitochondria.

**Knock down of mNHE1 from ventricular myocardium.** We also used biochemical approaches to assess NHE1 expression in mitochondria. We prepared mitochondrial fractions from 4-mo-old rat hearts and examined them for protein expression of NHE1 and Ca<sup>2+</sup>-induced mitochondrial swelling.

PPT.C.DsRed.H1.shNHE1 transduced hearts expressed the DsRed transgene product 14 days after vector transduction, whereas cardiomyocytes of sham-injected animals showed no fluorescence signals (Fig. 7A). DsRed labeling was seen in  $80 \pm 5\%$  of the rod-shaped cardiomyocytes attached to the cover slips ( $n = 1$ , 6 cover slips and  $\sim 250$  myocytes analyzed), which demonstrated the transduction efficiency of shRNA-NHE1 delivered by intramyocardial lentivirus injections. Left ventricular mitochondrial lysates were resolved by SDS-PAGE, blotted to polyvinylidene difluoride membranes, and probed with anti-NHE1 antibody or COXI antibody as loading controls (Fig. 7B). shRNA-NHE1 transduction reduced the expression of mNHE1 to  $26 \pm 13\%$  ( $n = 3$ ), compared with sham-injected ( $100 \pm 18\%$ ,  $n = 4$ ,  $P < 0.02$ ), in the rat heart (Fig. 7C). In another set of experiments, rats were injected with shRNA-NHE1 or a nonsilencing shRNA-SCR (scramble) in the left ventricular wall. One month after injection, NHE1 expression was analyzed in left ventricular mitochondrial lysates by Western blot (Fig. 7C). In this case, shRNA-NHE1 transduction reduced the expression of mNHE1 by  $46 \pm 14\%$

huNHE1 1 ERSKEPOLIAFYHKMEMKOA TELVESGGMGKIPSAVSTVSMONTHPKSLPSERIILPALS  
 huNHE6 1 -----AIFLGRAANIYPTISILLNLGR-----RSKIGSNFOHMMFAGLRGAMAFAL  
 huNHE7 1 -----GWNFOHMMFSGLRGAMAFAL  
 huNHE9 1 -FILGAFLAIFVARACNIYPTISFLLNLGR-----KOKIPWNFOHMMFSGLRGATAFAL  
 huNHE8 1 -----SHYTHHNLSPVTOILMOOTLRTVAFLCETCVFAFLGLSIFSFPHKFEISEFVI  
 huNHE2 1 -----HAIEMAETGMIS-----TVPTFASINDCREEKIRKVTS  
 rtNHE4 1 -----GITIGPLVRYLDVRKTNKK-----ESINEELHIRLMDHLKAGIEDVC  
 huNHE3 1 -----YLLRENVSAVCLDMOSLEORRRSIRDAEDMVTHHTILOOYLKPROEYKH  
 huNHE5 1 -----SFKSTKHNICFTKSKPRPRKTGRRKKDGVANAEATNGKHRGLGFQDTA

huNHE1 61 DKEEEIRKILRNNLOKTRORILRSYNRHTLVADPYEEAWNOMLLRROKAROLEOKINN---  
 huNHE6 47 AIRDTATYAROMMFSTTLLIVFFTWWVFGGCTTAMLSCLHIRVGVDSDOE-----  
 huNHE7 22 AIRDTASYAROMMFSTTLLIVFFTWWIIGGCTTMLSCLNIRVGVVEEPSEEDONEHHWOY  
 huNHE9 54 AIRNTESOPKOMMFSTTLLIVFFTWWVFGGCTTPLMTWLOTIRVGVLDLNLKEDPSS---  
 huNHE8 53 WCIVLVLFGRAVNIFPLSYLNFNRDHKITPKMMFIMMFSGLRCAIPYALSLH-----  
 huNHE2 34 SETDEIRELLSRNLYOIRORTLSYNRHSLTADTSEROAKEILIRRRHSLRESIRKDSSSLN  
 rtNHE4 43 GOWSHYOVRDKFKKFDHRYIRKILIRRNOPKSSIVSLYKLEMKOAIEMAETGLLSS---  
 huNHE3 50 LYSRHELTPTTEDEKODREIFHRTMRKRLESFKSTKIGLNONKKAALYKRERAKRR---  
 huNHE5 49 AVILTVSEEEEEESDSSETEKEDDEGIIFVARATSEVLOEGKVGSGSLEVCPSPRIIP--

huNHE1 118 -----YLTVPAHKLDSPTMSRARI GSDPLAYEFPKEDLPVITID  
 huNHE6 97 -----HLGVPENERRTTKAESAWLFRMWFYFDHNYLKPILLTHS  
 huNHE7 82 FRVGVDPDODPPPNND SFOVLOGDGPDSARGNRTKOESAWIFRLWYSFDHNYLKPILTHS  
 huNHE9 111 -----OHOEANNLDKNMTKAESARLFRMWFYFDHNYLKPILTHS  
 huNHE8 106 -----LDLEPMEKROLIGTTTIVITVLFVFTILLGGSTMPILRLM  
 huNHE2 94 -----REHRASTSTSRYSLPKNTKLEPKOKRRTISADGNSSD  
 rtNHE4 100 -----VASPTPYOSERIOGIKRI SPEDVESMRDIITRNMYOV  
 huNHE3 107 -----NSSIPNGKLPMESPAONFTIKEKDLLESDTEEPNYDE  
 huNHE5 107 -----PSPTCAEKELPWKSGQGD LAVYVSSETTKIVPVMQNT

huNHE1 156 --PASPOSPESVDLVNEELKGVKVLGSLRDPKVAEED-EDD-DGGIMMRSKETSSPGTDD  
 huNHE6 135 GPPLTTTLPACCGPIARCLTSPOAYENOEOLKDDSD-LILNDGDISLTYGDSTVNTPEA  
 huNHE7 142 GPPLTTTLPACCGPIARCLTSPOAYDNOEPLREEDSD-FILTEGDLTLYGDSTVTANGS  
 huNHE9 150 GPPLTTTLPACCGPIARCLTSPOAYG--EOLKEDDVE-CIIVNODELATNYOEOASSP---  
 huNHE8 144 DIEDAKAHRNKKDVNLSKTEKMGNTVESEHLSLTE-EEYEAHYIRRODLKGFVWLDK  
 huNHE2 134 SDADAGITVLNLOPRARRFLPEOFSKKSPOSYKMEWKNEVDVSDGRDMPSTPPTPHSREK  
 rtNHE4 137 RORTLSYNKYNLKPOTSEKOAKEILIRRONTLRESLR-KGOSLPWPKPAGTKNFRYLSFP  
 huNHE3 145 EMSGGIEFLASVTKDTASDSPAGIDNPVFSPEALDRSLIARLPPWLSPGETVVPSORAR  
 huNHE5 144 GWNQSISSLESIASPPCNQAPILTCCLPPHPRGTEEPQVPIHLPSPDRSSFAFPPLAKAG

huNHE1 212 VETPAP-----SDSPSSORIORCLSDFGPHPEPGE GEPFFPKGO-----  
 huNHE6 194 TSSAPR-----RFMGNSSEDALDRELAFGDHELVI RGLRVLPMDDSEPPNLNLLDNTR  
 huNHE7 201 SSSHTASTSLEGSRRTKSSSEEVLERDLGMDGOKVSSRGLRVLPLEDNA-----  
 huNHE9 204 CSPPARLGLDOKASPOTPGKENIYEGDLGLGGLG YELKLEOTLGOSOLN-----  
 huNHE8 203 YLNRFFTR---RLTOEDLHHGRIOMKTIITNKWYEEVROGSPSGEDDEOELL-----  
 huNHE2 194 GTOTSGLLOOPLLKDOSGSEEREDSLTEGIPPKPPRLVWRASEPGSRKARFGSEKP---  
 rtNHE4 196 YSNPOPARRGARA AESTGNPCCWLLHFLICRAMVEKIWGP GGOETOPRLLCRNLN-----  
 huNHE3 205 TOIPYSPGTFRRLMPFRLSSKSVDSFLOADGPEERPPAALPESTM-----  
 huNHE5 204 RSRSESSADLPQQQLQPLMGHKDHTHISPGTATSHWCIQFNRSRL-----

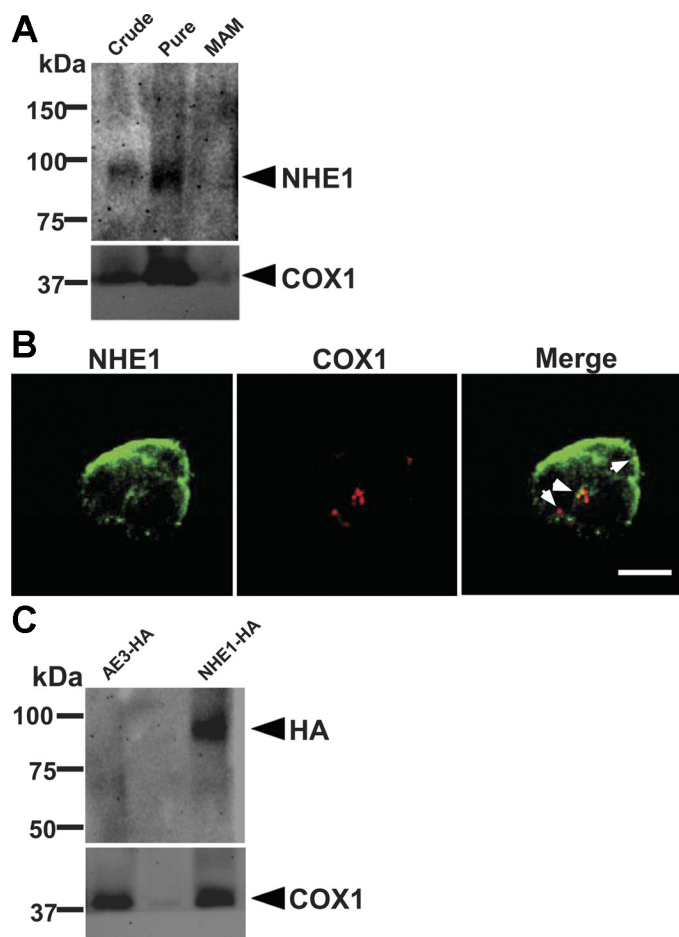


Fig. 5. Expression of NHE1 in Percoll-purified rat heart mitochondria and immunocytochemical and immunoblot analysis of the expression of NHE1, human hemagglutinin epitope-tagged NHE1 (NHE1-HA), and COX1 in HEK 293 cell lysates or HEK 293 cell mitochondrial lysates. *A*: 100  $\mu$ g of crude mitochondrial lysates, pure mitochondria lysates, and membrane-associated mitochondrial (MAM) lysate, obtained as explained in MATERIALS AND METHODS, were analyzed by 8% SDS-PAGE, transferred to PVDF membranes, and probed with antibodies indicated by the arrows against NHE1 or COX1. *B*: HEK 293 cells plated on glass cover slips were double stained as indicated on *top* with rabbit anti-NHE1 antibody, followed by Alexa Fluor 488-conjugated chicken anti-rabbit IgG secondary antibody (AE3, green) and with mouse anti-COX1 antibody, followed by Alexa Fluor 594-conjugated chicken anti-goat IgG (COX1, red). Images were collected with a Zeiss LSM-410 laser-scanning confocal microscope. Colocalization of NHE1 and COX1 is indicated as a merged image and with yellow/orange staining and arrowheads. Scale bar = 10  $\mu$ m. *C*: mitochondrial lysates prepared from HEK 293 cells transfected with AE3f-HA or HA-tagged NHE1 cDNAs were immunoblotted and probed for the expression of AE3f-HA or NHE1-HA with anti-HA antibodies (*top*) or probed for the expression of COX1 (*bottom*).

( $n = 4$ ), compared with shRNA-SCR-transduced ( $100 \pm 11\%$ ,  $n = 3$ ,  $P < 0.05$ ), in the rat heart (Fig. 7D). The efficiency of NHE1 reduction in the myocardium upon shRNA-NHE1 transduction was further investigated in pure membrane preparations isolated from left ventricular muscle of rats injected with

shRNA-SCR or shRNA-NHE1. One month after transduction, membrane NHE1 expression was also reduced by  $55 \pm 7\%$  ( $n = 4$ ) in rats transduced with shRNA-NHE1 compared with shRNA-SCR-transduced rats ( $100 \pm 7\%$ ,  $n = 3$ ). Therefore, we corroborated that transduction of shRNA-NHE1 in the rat myocardium has the ability to reduce the expression of mNHE1 and membrane NHE1 to the same extent.

We conclude that stable expression of shRNA-NHE1 delivered with a lentiviral-based vector system significantly reduced the expression of NHE1 protein in mitochondria. Thus we confirmed the expression of the NHE1 Na<sup>+</sup>/H<sup>+</sup> exchanger in the subcellular organelle.

**Functional role of NHE1 in mitochondria.** Induction of the MPTP has been implicated in cellular apoptosis and in I/R injury. Shortly after myocardial ischemia, the MPTP, a channel in mitochondrial membrane, opens and causes isolated mitochondria to swell. Measurements of Ca<sup>2+</sup>-induced mitochondrial swelling were initially tested here in deenergized mitochondria isolated from rat hearts transduced with either shRNA-SCR or shRNA-NHE1 (Fig. 8A). Step addition of 50  $\mu$ M CaCl<sub>2</sub> induced a small decrease in light scattering, at each step, in shRNA-SCR-transduced rats that was attenuated by the NHE1 inhibitor HOE-642 (10  $\mu$ M, cariporide). The decrease in light scattering was, however, blunted in shRNA-NHE1-transduced animals, and no additional effect was observed with the addition of cariporide. To characterize further the role of NHE1 in mitochondria, animals were transduced with shRNA-SCR (nonsilencing control,  $n = 3$ ), or transduced with shRNA-NHE1 ( $n = 4$ ). One month after transduction, mitochondria were isolated from left ventricular myocardium, and mitochondrial suspensions were exposed to 200  $\mu$ M CaCl<sub>2</sub>, which is known to induce MPTP opening with the consequent mitochondrial swelling (6, 21) (Fig. 8, B and C). If the MPTP is open after the Ca<sup>2+</sup> addition, solutes will be free to enter the matrix, causing the mitochondria to swell. These changes are observed as decreases in light scattering. Light scattering decrease was calculated for each sample by taking the difference between the values before and after the addition of CaCl<sub>2</sub>. The decrease in light scattering induced by Ca<sup>2+</sup> addition to mitochondria is used as an indication of mitochondrial swelling. In rats transduced with shRNA-SCR, addition of 200  $\mu$ M CaCl<sub>2</sub> evoked a large decrease in light scattering (Fig. 8B). Conversely, rats transduced with shRNA-NHE1 showed little decrease in light scattering and a significant reduction in mitochondrial swelling,  $36 \pm 4\%$  (7 mitochondrial suspensions), compared with scrambled control,  $100 \pm 4\%$  (6 mitochondrial suspensions). Interestingly, inhibition of NHE1 with cariporide decreased Ca<sup>2+</sup>-induced mitochondrial swelling in rats transduced with shRNA-SCR,  $63 \pm 6\%$  (4 mitochondrial suspensions), providing evidence for a direct mitochondrial action of the NHE1. Cariporide did not, however, further decrease mitochondrial swelling in rats transduced with shRNA-NHE1,  $33 \pm 6\%$  (3 mitochondrial suspensions). Fail-

Fig. 4. Multiple sequence alignment of human (hu) NHE proteins and rat nhe4 ortholog. Comparison of the amino acid sequences of the cytoplasmic COOH terminus of human NHE1-NHE3 and NHE5-NHE9 (GenBank<sup>TM</sup> accession nos. NP\_003038, NP\_003039, NP\_004165 and NP\_004585, NP\_001036002, NP\_115980, NP\_056081, BAD69592, respectively) or rat nhe4 (NP\_775121) was rendered using the CLUSTAL W multiple sequence alignment algorithm (<http://align.genome.jp/>). Gaps (indicated by broken line) were introduced in the sequence to maintain the alignment. Positions containing identical residues are shaded in black while conservative amino acid differences are shaded in gray. Bars above text indicate sequence of NHE1 epitopes recognized by mouse anti-NHE1 antibody (black), Rb a-NHE1 antibody (gray), and goat a-NHE1 antibody (white).

Table 1. Prediction of mitochondrial targeting sequences

Gene	Common Name	Cleavage Site	Probability of Export to Mitochondria
SLC9A1	NHE1	MVLRSGICGLSPHRIFPSSLVVVALVGLLPVLR	0.859
SLC9A2	NHE2	MEPLGNWRSRLRAPLPPMLLLLLLQVAGPVGALAEETLLNAPA	0.084
SLC9A3	NHE3	MWGLGARGPDRGLLALALGGLARA	0.588
SLC9A4	NHE4	Not predictable	0.217
SLC9A5	NHE5	Not predictable	0.077
SLC9A6	NHE6	MARRGWRRAPLRRG	0.996
SLC9A7	NHE7	Not predictable	0.024
SLC9A8	NHE8	Not predictable	0.008
SLC9A9	NHE9	Not predictable	0.019
SLC9A10	NHE10	Not predictable	0.145
MT-CO1	COX1	MLATRVFSLVGKRAISTSVQVR	0.981
ATP1A2	Na <sup>+</sup> -K <sup>+</sup> -ATPase α <sub>2</sub>	Not predictable	0.321

NHE, Na<sup>+</sup>/H<sup>+</sup> exchanger; COX1, cytochrome *c* oxidase complex I. NH<sub>2</sub>-terminal protein regions supporting a mitochondrial targeting sequence and their cleavage site obtained with the MITOPROT Software (<http://ihg2.helmholtzmuenchen.de/ihg/mitoprot.html>). Protein sequences were retrieved from the SwissProt Database.

ure of cariporide to induce additional decrease in mitochondrial swelling in rats with reduced NHE1 expression allowed us to conclude that NHE1 is indeed expressed in the mitochondria.

To demonstrate the effectiveness of classical MPTP blockers (28), mitochondrial suspensions from rats transduced with shRNA-SCR, or rats transduced with shRNA-NHE1, were exposed to 400 μM CaCl<sub>2</sub> in the presence of the MPTP inhibitor cyclosporin A (CsA, 1 μM) [Supplemental Fig. 1 (Supplemental data for this article may be found on the *American Journal of Physiology: Heart and Circulatory Physiology* website.)]. Mitochondrial suspensions displayed no decrease in light scattering in Ca<sup>2+</sup>-free solution under the same experimental conditions described above (Supplemental Fig. 1A). As expected, the MPTP inhibitor CsA significantly decreased Ca<sup>2+</sup>-induced mitochondrial swelling in rats transduced with shRNA-SCR, suggesting that the increase in mitochondrial volume was attributable to the MPTP opening. Interestingly, in rats transduced with shRNA-NHE1, the decrease in mitochondrial swelling after the exposure to 400 μM CaCl<sub>2</sub> was similar with or without blockade of the MPTP with CsA. Because CsA did not further decrease Ca<sup>2+</sup>-induced mitochondrial swelling in rats with low levels of mNHE1 expression, we speculate that NHE1 plays a key role in the mitochondrial function and integrity (Supplemental Fig. 1B).

Table 2. Prediction of mitochondrial targeting sequences

NHE1 and nhe1 Orthologs	Cleavage Site	Probability of Export to Mitochondria
hu NHE1	MVLRSGICGLSPHRIFPSSLVVVALVGLLPVLR	0.859
rt nhe1	MMLRWSGIWGLYPPRIFPSSLVVVALVGLLPVLR	0.693
rb nhe1	MLLWSAVRGLSPPRIVPSSLVVVALAGLLPGLR	0.892
mo nhe1	MMLRWSGVWGFPPRIFPSSLVVVALVGLLPVLR	0.546
pg nhe1	MLLWSGICGLSPPRIFPSSLVVVALVGLLPVLR	0.529
sl nhe1	Not predictable.	0.860
br nhe1	MGAAALRALPWALLLLGPLLPGQRL	0.462
fs nhe1	MAALLLRAPRSSSSSGRSAARLAGLLACVLLLLAAGASASRD	0.963

NH<sub>2</sub>-terminal protein regions supporting a mitochondrial targeting sequence and their cleavage site obtained with the MITOPROT Software (<http://ihg2.helmholtzmuenchen.de/ihg/mitoprot.html>). Protein sequences were retrieved from the SwissProt Database. hu, Human (*Homo sapiens*); rt, rat (*Rattus norvegicus*); rb, rabbit (*Oryctolagus cuniculus*); mo, mouse (*Mus musculus*); pg, pig (*Sus scrofa*); sl, salamander (*Amphiuma tridactylum*); br, bird (*Gallus gallus*); fs, fish (*Pseudopleuronectes americanus*).

We conclude that NHE1 plays a functional role in heart mitochondria and that the MPTP opening and subsequent mitochondrial volume increase triggered by CaCl<sub>2</sub> is due, at least in part, to the mNHE1.

mNHE1 would catalyze the H<sup>+</sup> influx into the mitochondria, regulating mitochondrial matrix pH homeostasis, playing a role in mitochondrial metabolism, and being a factor in determining MPTP opening. Although we have not ruled out the expression of NHE6 (MITOPROT analysis, Table 1), the NHE1 seems to be the isoform involved in the delay of the MPTP opening.

## DISCUSSION

In 1969, Mitchell and Moyle (42) proposed the existence of Na<sup>+</sup>/H<sup>+</sup> exchange in mitochondria and Garlid et al. (24) in 1991 demonstrated in beef heart mitochondria that solubilized NHE in the organelle can be purified in an active state. In mitochondria, NHE mediates the exchange of matrix Na<sup>+</sup> for intermembrane H<sup>+</sup> generated by respiration (23). Thus H<sup>+</sup> influx in the mitochondrial matrix through the mitochondrial NHE would constitute a form of H<sup>+</sup> leakage not coupled to ATP synthesis, which in turn will dissipate the energy stored as transmembrane H<sup>+</sup> gradient.

NHE1 is a typical integral membrane protein with 10–12 predicted spanning segments, a long COOH terminus, and an

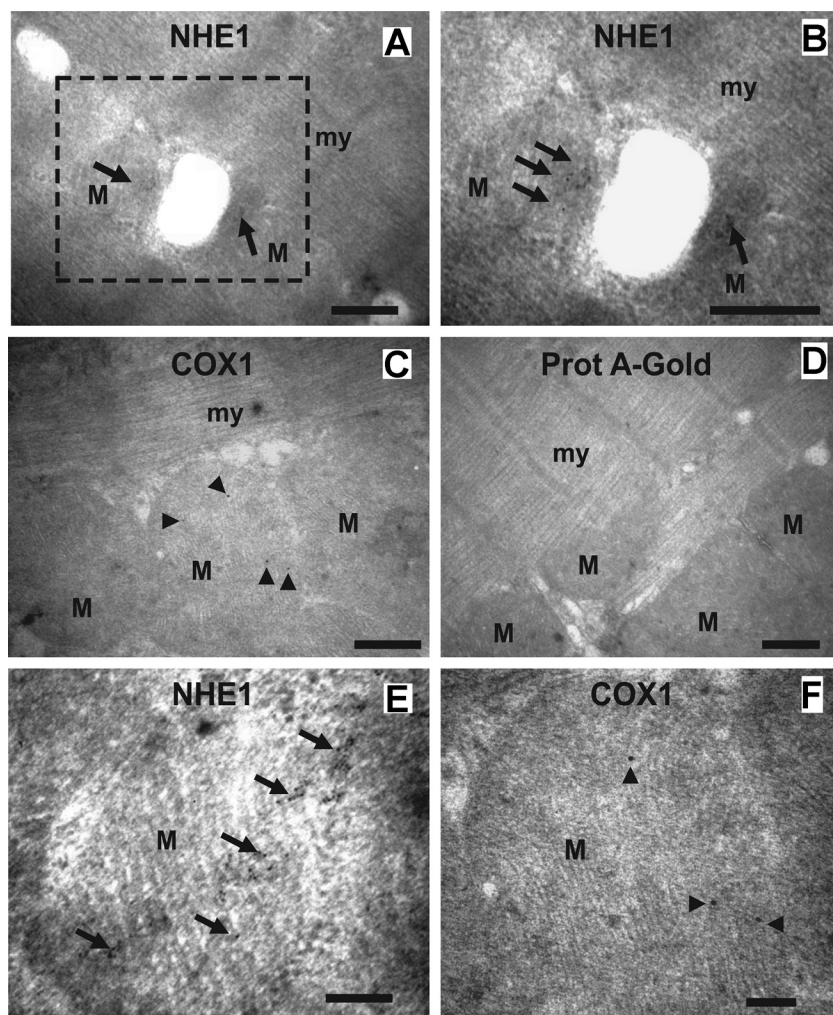


Fig. 6. Subcellular location of NHE1 and COXI in heart muscle sections. Different magnifications of left ventricular rat papillary muscle sections labeled with anti-NHE1 antibody (A, B, and E) or anti-COXI antibody (C and F), followed by incubation with protein A conjugated to 14-nm gold particles, or muscle section labeled only with protein A-gold conjugated (D). B: Zoomed image of dashed-square delimited area indicated in A. Arrows show gold particles corresponding to labeling of NHE1 in mitochondria (M), whereas arrowheads display labeling of gold particles corresponding to COXI. Bars = 500 nm (A-D) and 200 nm (E and F). my, Myofilaments.

NH<sub>2</sub>-terminal tail that poses the mitochondrial localization signal. Besides the expression of NHE1 in the plasma membrane of cardiac cells, herein we have characterized the expression of NHE1 in mitochondria of cardiac muscle. Recently, the expression of NHE1 was suggested in Percoll-purified rat heart mitochondria by immunoblot analysis (32).

In addition to characterizing the localization of NHE1 in the heart mitochondria, we report one major functional role: the increase in threshold to open the MPTP in rat heart deficient in NHE1.

The dual localization pattern displayed by NHE1 is somehow surprising although not unique among other membrane proteins. Other studies have reported the presence of Kv1.3 (53), Kir6.2 (22), and Ca<sup>2+</sup>-activated BK potassium channels (51), NCX1–3 (25), and CX43 (8, 9) in the plasma and mitochondrial membranes. Unlike NHE1 (MITOPROT Software, Tables 1 and 2), all of these channels did not exhibit classical basic NH<sub>2</sub>-terminal mitochondrial targeting presequences but are targeted to mitochondrial inner membranes by unknown mechanisms. Several mitochondrial proteins of the inner membrane characterized by many highly hydrophobic transmembrane segments, similarly to NHE1, and that lack the NH<sub>2</sub>-terminal sequence become imported into the mitochondria in a Tim22 complex-dependent pathway (56). The sorting

and targeting information seems to comprise several distant amino acids spread throughout the mature protein and is hardly recognizable (11, 17). Although specific posttranslational protein modifications and differential splicing have been considered to account for organellar protein targeting, the mechanisms responsible for the simultaneous targeting of a protein (NHE1) to different cellular compartments (plasma membrane, mitochondria) are not known and are beyond the focus of the present study.

Emerging evidence supports the fact that mitochondrial dysfunction underlies the causes of numerous cardiac diseases [for review, see Baines (5)]. Studies on the MPTP and its role in reperfusion injury and cardiac hypertrophy have proven fruitful (27, 45). Griffith and Hallestrap (26) and Duchon et al. (18) first showed that delayed opening of MPTP by CsA protects I/R injury in perfused rat hearts. Recently, Piot et al. (45) reported in humans with acute myocardial infarction the decrease in infarct size by the MPTP inhibitor CsA administered at the time of reperfusion. Interestingly, a role of mitochondria in determining cardiac hypertrophy after myocardial infarction has also been proposed (12, 15, 30, 33, 34).

NHE1 inhibition was one of the most promising therapeutic strategies for I/R injury based on experimental animal studies.

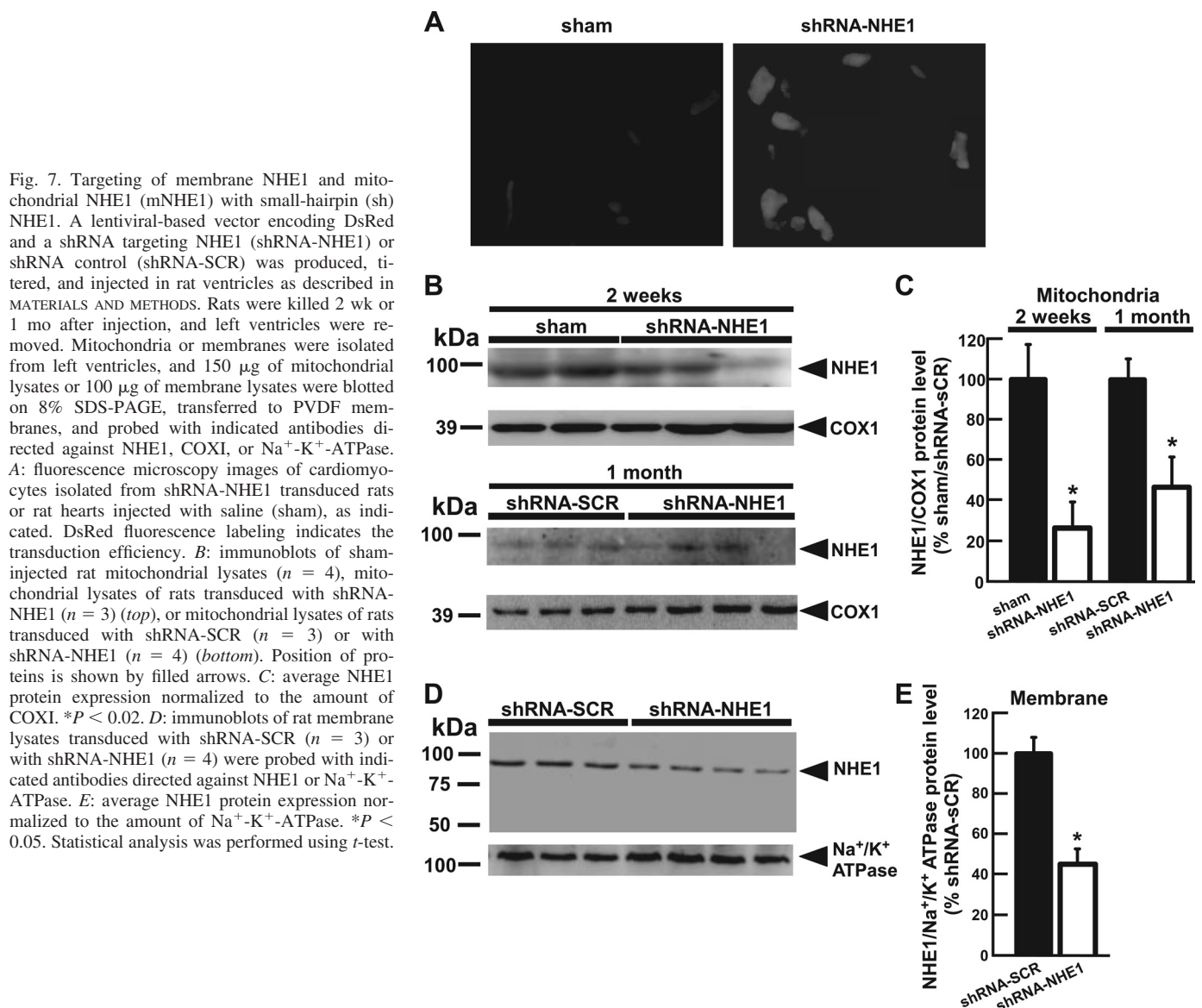


Fig. 7. Targeting of membrane NHE1 and mitochondrial NHE1 (mNHE1) with small-hairpin (sh) NHE1. A lentiviral-based vector encoding DsRed and a shRNA targeting NHE1 (shRNA-NHE1) or shRNA control (shRNA-SCR) was produced, titrated, and injected in rat ventricles as described in MATERIALS AND METHODS. Rats were killed 2 wk or 1 mo after injection, and left ventricles were removed. Mitochondria or membranes were isolated from left ventricles, and 150  $\mu\text{g}$  of mitochondrial lysates or 100  $\mu\text{g}$  of membrane lysates were blotted on 8% SDS-PAGE, transferred to PVDF membranes, and probed with indicated antibodies directed against NHE1, COX1, or  $\text{Na}^+/\text{K}^+$ -ATPase. A: fluorescence microscopy images of cardiomyocytes isolated from shRNA-NHE1 transduced rats or rat hearts injected with saline (sham), as indicated. DsRed fluorescence labeling indicates the transduction efficiency. B: immunoblots of sham-injected rat mitochondrial lysates ( $n = 4$ ), mitochondrial lysates of rats transduced with shRNA-NHE1 ( $n = 3$ ) (top), or mitochondrial lysates of rats transduced with shRNA-SCR ( $n = 3$ ) or with shRNA-NHE1 ( $n = 4$ ) (bottom). Position of proteins is shown by filled arrows. C: average NHE1 protein expression normalized to the amount of COX1.  $*P < 0.02$ . D: immunoblots of rat membrane lysates transduced with shRNA-SCR ( $n = 3$ ) or with shRNA-NHE1 ( $n = 4$ ) were probed with indicated antibodies directed against NHE1 or  $\text{Na}^+/\text{K}^+$ -ATPase. E: average NHE1 protein expression normalized to the amount of  $\text{Na}^+/\text{K}^+$ -ATPase.  $*P < 0.05$ . Statistical analysis was performed using *t*-test.

Controversial results, however, were obtained using NHE1 inhibitors in clinical trials: cariporide (GUARDIAN) (55) or EXPEDITION (41) and Eniporide (ESCAMI) (59) [for review, see Murphy and Allen (43)]. These trials were unable to demonstrate a significant reduction in mortality when these compounds were tested in patients after acute myocardial infarction (55, 59) or were suspended early due to undesired cerebrovascular side effects (41). Yet, in a subgroup of patients who underwent coronary artery bypass graft surgery, a 25% improvement in cardiac performance was detected with cariporide. Similar beneficial effects were seen in a small trial of 100 patients who received cariporide before percutaneous coronary angioplasty (49).

The related myocardial protective effects induced by cyclosporine and NHE1 inhibition prompted us to speculate about the possibility that NHE1 inhibition protects the heart by targeting previously primed mitochondria (46).

Since the seminal paper by Karmazyn (34) showing that NHE1 inhibition protects the isolated heart from I/R injury,

followed by numerous experimental studies (19, 37, 57), and ending in clinical trials (49, 55), the effects of NHE1 inhibition were analyzed without considering a mitochondrial effect. Only a report by Ruiz Meana et al. (48) drew attention to this possibility. In connection with this, Teshima and collaborators (54) demonstrated that cariporide protects cardiomyocyte death induced by oxidative stress, preventing cytosolic  $\text{Na}^+$  and  $\text{Ca}^{2+}$  accumulation and mitochondrial  $\text{Ca}^{2+}$  overload, and preserving mitochondrial  $\Delta\Psi_m$ . Although these effects were proposed to be secondary to prevention of the cytosolic increase in  $\text{Ca}^{2+}$ , more recently a direct mitochondrial action of NHE1 inhibitors, which decrease myocardial superoxide production, was reported (21). A “cyclosporine like effect” of NHE1 inhibition was proposed, but the site of action of those compounds was not identified (21).

A mitochondrial action of NHE1 inhibition secondary to changes in cytosol was previously reported by Javadov et al. (31). Those authors were unable to detect changes in isolated mitochondria perhaps because of the controlled  $\text{Ca}^{2+}$

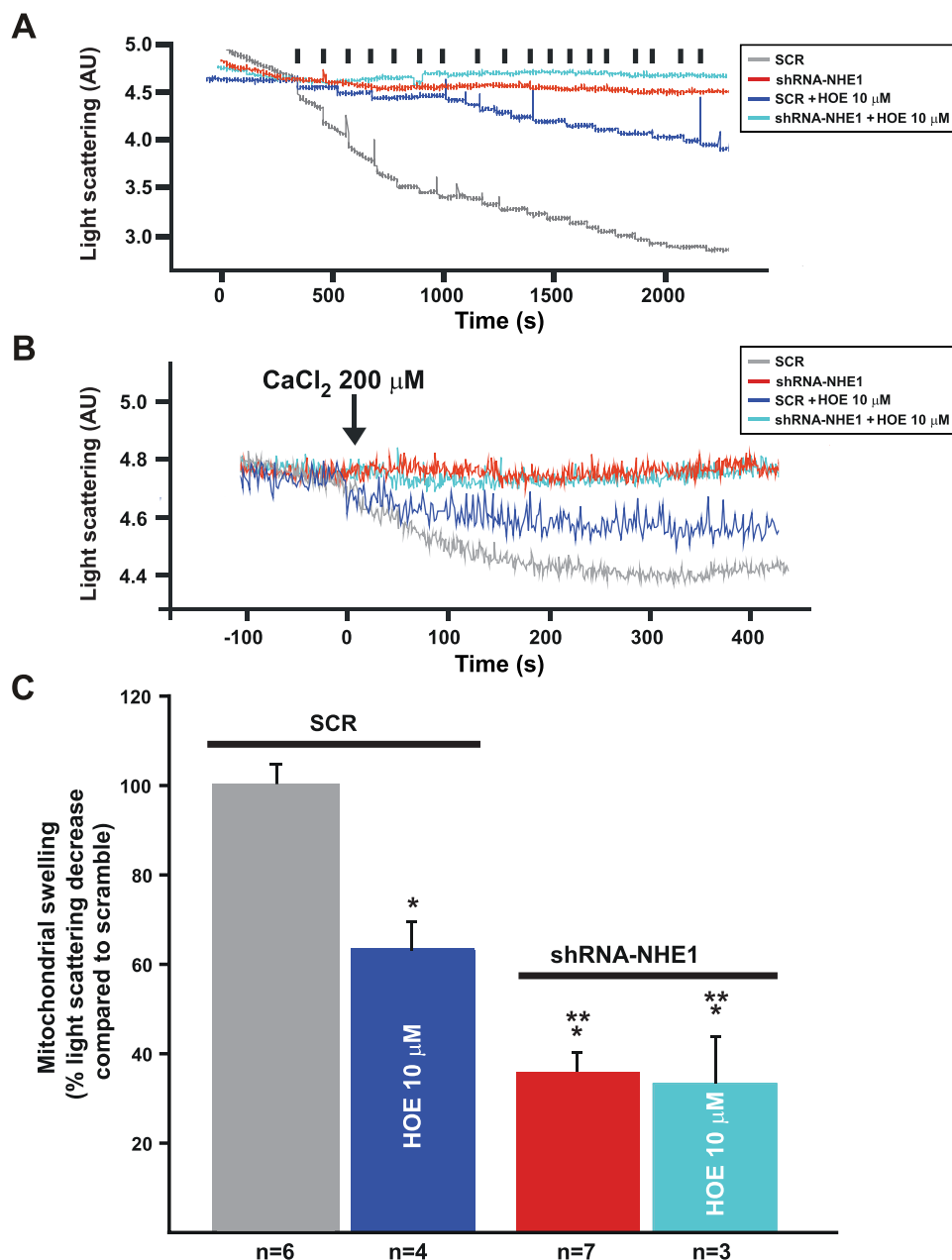


Fig. 8. CaCl<sub>2</sub>-induced swelling of rat heart mitochondria. *A*: sample scattered light absorbance traces of Ca<sup>2+</sup>-induced swelling in response to step addition of CaCl<sub>2</sub> (50  $\mu$ M, bars over text) for heart mitochondria isolated from rats transduced with shRNA-NHE1 or with shRNA-SCR (SCR, scrambled, control) in the presence or absence of cariporide (HOE-642, 10  $\mu$ M). *B*: typical experiment showing that shRNA-NHE1 transduction (3 rats, 7 mitochondrial suspensions) significantly inhibited Ca<sup>2+</sup>-induced mitochondrial swelling and the decrease in light scattering of mitochondrial suspensions compared with SCR-transduced animals (3 rats, 6 mitochondrial suspensions). Cariporide attenuated the decrease in light scattering in SCR-transduced rats (3 rats, 4 mitochondrial suspensions) and did not affect the decrease in light scattering in shRNA-NHE1-transduced rats (3 rats, 3 mitochondrial suspensions). *C*: summary results of light scattering decrease in rats transduced with shRNA-SCR or with shRNA-NHE1, before and after treatment with 10  $\mu$ M HOE-642. The fact that shRNA-NHE1 have a more profound effect on mitochondrial swelling compared with 10  $\mu$ M HOE suggests that probably the HOE dose used here was not sufficient to achieve maximal inhibition. \**P* < 0.05 vs. SCR and \*\**P* < 0.05 vs. SCR + 10  $\mu$ M HOE-642 (ANOVA).

gradients in the mitochondria and suggested an action on MPTP function through glycogen synthase kinase 3 $\beta$  (33). Although we cannot rule out changes in this kinase, our similar and not additive results obtained in isolated mitochondria with inhibition and silencing of the mNHE1 limit the discussion.

We have demonstrated that we were able to knock down the expression of NHE1 expressed in membrane fractions of either sarcolemmal or mitochondrion by direct intramyocardial injec-

tions of shRNA-NHE1 in rats (Fig. 7). Intramyocardial injection of lentivirus carrying a shRNA-NHE1 not only reduced the expression of NHE1 at the level of mitochondria but also prevented Ca<sup>2+</sup>-induced swelling of rat heart mitochondria (Figs. 7 and 8 and Supplemental Fig. 1).

A decrease in mitochondrial exchanger function (or reduced expression by siRNA) should increase H<sup>+</sup> concentration on the external side of the MPTP. In connection with this, the pre-

vention of MPTP formation by acidosis in reperfusion after ischemia has been reported (16, 47). MPTP opening can be further increased when Ca<sup>2+</sup> overload is associated by oxidative stress. Moreover, a decrease in mitochondrial anion superoxide production induced by two known enhancers of reactive oxygen species (ROS) production, ANG II and endothelin-1, upon NHE1 inhibition has been reported (21). Furthermore, the increase in ROS production induced by the opening of mitochondrial ATP-dependent K<sup>+</sup> was abolished by cariporide (21).

We are reporting a delay of MPTP formation in isolated mitochondria by NHE1 inhibition and posttranscriptional NHE1 gene silencing. These findings open a new avenue of research about the mechanism of protection achieved by NHE1 inhibition either in reperfusion injury or in cardiac hypertrophy and failure.

#### GRANTS

This work was supported by Proyecto de Investigación Científica y Tecnológica (PICT) 2007 no. 01011 Fondo para la Investigación Científica y Tecnológica (FONCyT, Argentina) Grant to B. V. Alvarez and PICT no. 05-38057 (FONCyT, Argentina) Grant to H. E. Cingolani. E. Cingolani was supported by a Cedars Sinai Medical Center/Sports Spectacular Research Award.

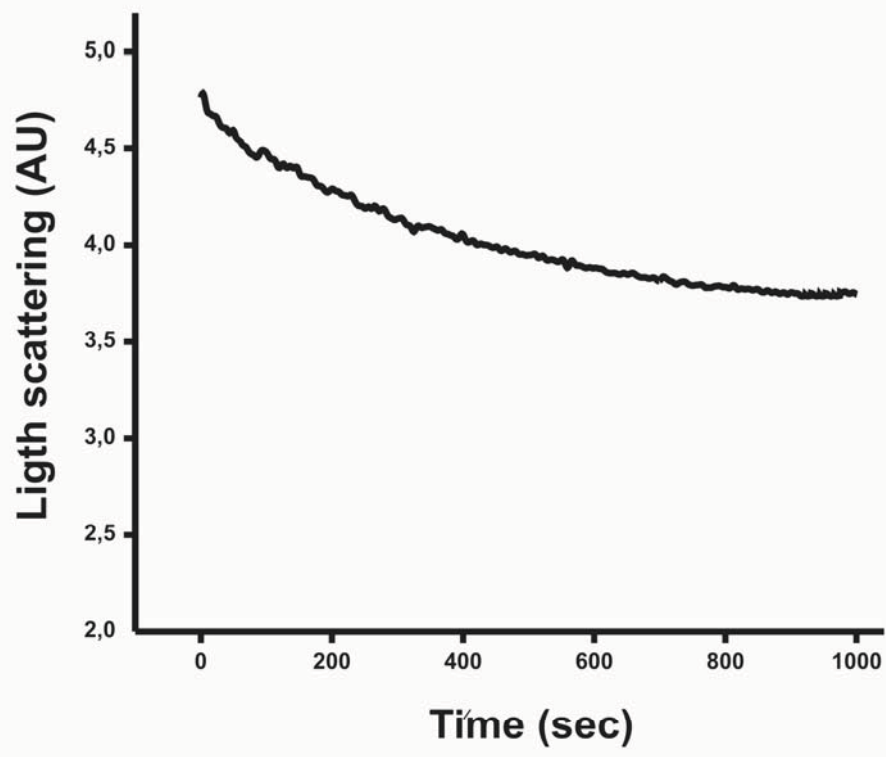
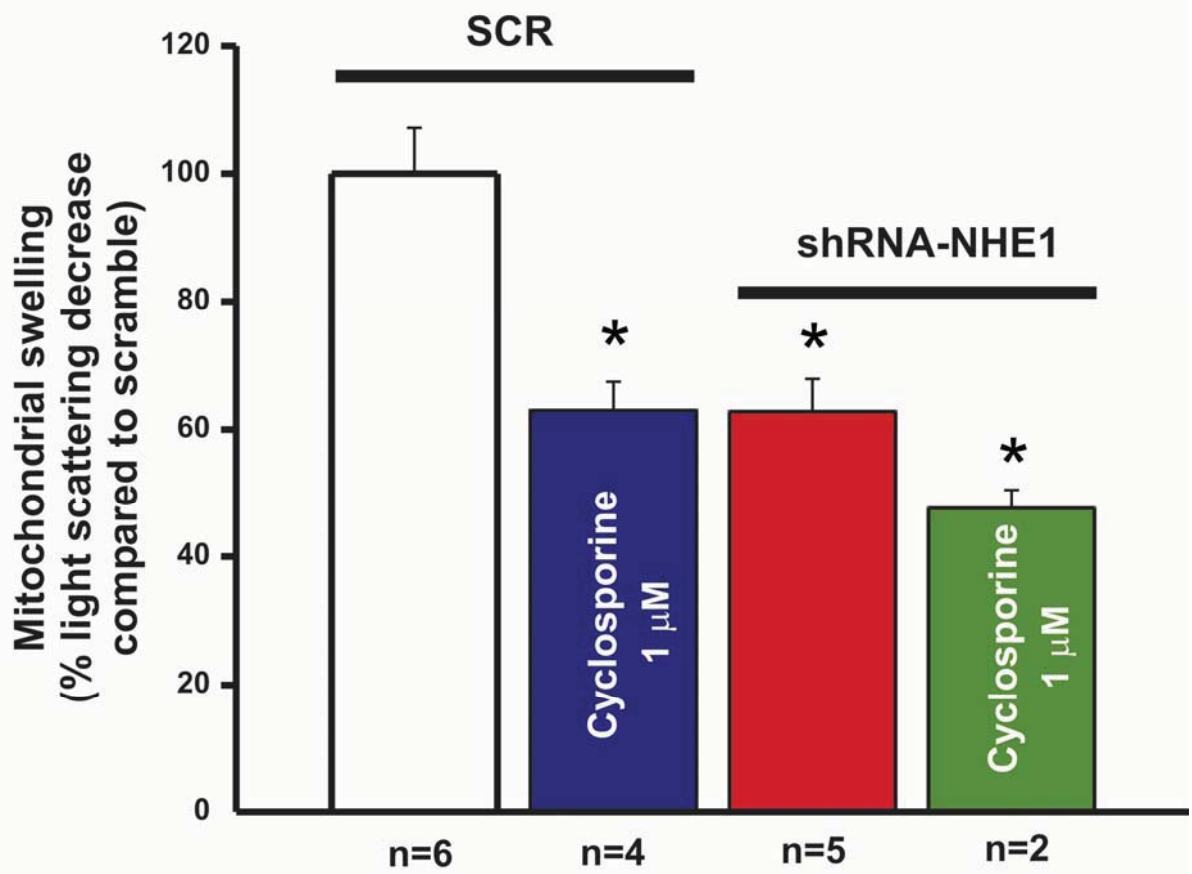
#### DISCLOSURES

None.

#### REFERENCES

- Akram S, Teong HF, Fliegel L, Pervaiz S, Clement MV. Reactive oxygen species-mediated regulation of the Na<sup>+</sup>-H<sup>+</sup> exchanger 1 gene expression connects intracellular redox status with cells' sensitivity to death triggers. *Cell Death Differ* 13: 628–641, 2006.
- Alvarez BV, Johnson DE, Sowah D, Soliman D, Light PE, Xia Y, Karmazyn M, Casey JR. Carbonic anhydrase inhibition prevents and reverts cardiomyocyte hypertrophy. *J Physiol* 579: 127–145, 2007.
- Alvarez BV, Kieller DM, Quon AL, Robertson M, Casey JR. Cardiac hypertrophy in anion exchanger 1-null mutant mice with severe hemolytic anemia. *Am J Physiol Heart Circ Physiol* 292: H1301–H1312, 2007.
- Avkiran M. Rational basis for use of sodium-hydrogen exchange inhibitors in myocardial ischemia. *Am J Cardiol* 83: 10G–18G, 1999.
- Baines CP. The cardiac mitochondrion: nexus of stress. *Annu Rev Physiol* 72: 61–80, 2010.
- Baines CP, Song CX, Zheng YT, Wang GW, Zhang J, Wang OL, Guo Y, Bolli R, Cardwell EM, Ping P. Protein kinase Cepsilon interacts with and inhibits the permeability transition pore in cardiac mitochondria. *Circ Res* 92: 873–880, 2003.
- Barth AS, Kizana E, Smith RR, Terrovitis J, Dong P, Leppo MK, Zhang Y, Miake J, Olson EN, Schneider JW, Abraham MR, Marban E. Lentiviral vectors bearing the cardiac promoter of the Na<sup>+</sup>-Ca<sup>2+</sup> exchanger report cardiogenic differentiation in stem cells. *Mol Ther* 16: 957–964, 2008.
- Boengler K, Dodoni G, Rodriguez-Sinovas A, Cabestrero A, Ruiz-Meana M, Gres P, Konietzka I, Lopez-Iglesias C, Garcia-Dorado D, Di Lisa F, Heusch G, Schulz R. Connexin 43 in cardiomyocyte mitochondria and its increase by ischemic preconditioning. *Cardiovasc Res* 67: 234–244, 2005.
- Boengler K, Stahlhofen S, van de Sand A, Gres P, Ruiz-Meana M, Garcia-Dorado D, Heusch G, Schulz R. Presence of connexin 43 in subsarcolemmal, but not in interfibrillar cardiomyocyte mitochondria. *Basic Res Cardiol* 104: 141–147, 2009.
- Brett CL, Wei Y, Donowitz M, Rao R. Human Na<sup>+</sup>/H<sup>+</sup> exchanger isoform 6 is found in recycling endosomes of cells, not in mitochondria. *Am J Physiol Cell Physiol* 282: C1031–C1041, 2002.
- Brix J, Rudiger S, Bukau B, Schneider-Mergener J, Pfanner N. Distribution of binding sequences for the mitochondrial import receptors Tom20, Tom22, and Tom70 in a presequence-carrying preprotein and a non-cleavable preprotein. *J Biol Chem* 274: 16522–16530, 1999.
- Caldiz CI, Garcarena CD, Dulce RA, Novareto LP, Yeves AM, Ennis IL, Cingolani HE, Chiappe de Cingolani G, Perez NG. Mitochondrial reactive oxygen species activate the slow force response to stretch in feline myocardium. *J Physiol* 584: 895–905, 2007.
- Casey JR, Sly WS, Shah GN, Alvarez BV. Bicarbonate homeostasis in excitable tissues: role of AE3 Cl<sup>-</sup>/HCO<sub>3</sub><sup>-</sup> exchanger and carbonic anhydrase XIV interaction. *Am J Physiol Cell Physiol* 297: C1091–C1102, 2009.
- Cingolani E, Ramirez Correa GA, Kizana E, Murata M, Cho HC, Marban E. Gene therapy to inhibit the calcium channel beta subunit: physiological consequences and pathophysiological effects in models of cardiac hypertrophy. *Circ Res* 101: 166–175, 2007.
- Cingolani HECC, Garcarena CD, De Giusti VC, Correa MV, Villa-Abrille MC, Yeves AM, Ennis IL, Chiappe de Cingolani G, Aiello EA. Early hypertrophic signals after myocardial stretch. Role of reactive oxygen species and the sodium/hydrogen exchanger. In: *Mechanosensitivity in Cells and Tissues: Mechanosensitivity of the Heart*, edited by Akai K. Moscow:Springer, 2010.
- Cohen MV, Yang XM, Downey JM. The pH hypothesis of postconditioning: staccato reperfusion reintroduces oxygen and perpetuates myocardial acidosis. *Circulation* 115: 1895–1903, 2007.
- Davis AJ, Ryan KR, Jensen RE. Tim23p contains separate and distinct signals for targeting to mitochondria and insertion into the inner membrane. *Mol Biol Cell* 9: 2577–2593, 1998.
- Duchen MR, McGuinness O, Brown LA, Crompton M. On the involvement of a cyclosporin A sensitive mitochondrial pore in myocardial reperfusion injury. *Cardiovasc Res* 27: 1790–1794, 1993.
- Fantinelli JC, Cingolani HE, Mosca SM. Na<sup>+</sup>/H<sup>+</sup> exchanger inhibition at the onset of reperfusion decreases myocardial infarct size: role of reactive oxygen species. *Cardiovasc Pathol* 15: 179–184, 2006.
- Fliegel L. Molecular biology of the myocardial Na<sup>+</sup>/H<sup>+</sup> exchanger. *J Mol Cell Cardiol* 44: 228–237, 2008.
- Garcarena CD, Caldiz CI, Correa MV, Schinella GR, Mosca SM, Chiappe de Cingolani GE, Cingolani HE, Ennis IL. Na<sup>+</sup>/H<sup>+</sup> exchanger-1 inhibitors decrease myocardial superoxide production via direct mitochondrial action. *J Appl Physiol* 105: 1706–1713, 2008.
- Garg V, Hu K. Protein kinase C isoform-dependent modulation of ATP-sensitive K<sup>+</sup> channels in mitochondrial inner membrane. *Am J Physiol Heart Circ Physiol* 293: H322–H332, 2007.
- Garlid KD. Sodium/proton antiporters in the mitochondrial inner membrane. *Adv Exp Med Biol* 232: 37–46, 1988.
- Garlid KD, Shariat-Madar Z, Nath S, Jezek P. Reconstitution and partial purification of the Na<sup>+</sup>-selective Na<sup>+</sup>/H<sup>+</sup> antiporter of beef heart mitochondria. *J Biol Chem* 266: 6518–6523, 1991.
- Gobbi P, Castaldo P, Minelli A, Salucci S, Magi S, Corcione E, Amoroso S. Mitochondrial localization of Na<sup>+</sup>/Ca<sup>2+</sup> exchangers NCX1–3 in neurons and astrocytes of adult rat brain in situ. *Pharmacol Res* 56: 556–565, 2007.
- Griffiths EJ, Halestrap AP. Protection by Cyclosporin A of ischemia/reperfusion-induced damage in isolated rat hearts. *J Mol Cell Cardiol* 25: 1461–1469, 1993.
- Halestrap AP, Pasdois P. The role of the mitochondrial permeability transition pore in heart disease. *Biochim Biophys Acta* 1787: 1402–1415, 2009.
- Heusch G, Boengler K, Schulz R. Inhibition of mitochondrial permeability transition pore opening: the Holy Grail of cardioprotection. *Basic Res Cardiol* 105: 151–154, 2010.
- Hill JK, Brett CL, Chyou A, Kallay LM, Sakaguchi M, Rao R, Gillespie PG. Vestibular hair bundles control pH with (Na<sup>+</sup>, K<sup>+</sup>)/H<sup>+</sup> exchangers NHE6 and NHE9. *J Neurosci* 26: 9944–9955, 2006.
- Javadov S, Choi A, Rajapurohitam V, Zeidan A, Basnakan AG, Karmazyn M. NHE-1 inhibition-induced cardioprotection against ischemia/reperfusion is associated with attenuation of the mitochondrial permeability transition. *Cardiovasc Res* 77: 416–424, 2008.
- Javadov S, Huang C, Kirshenbaum L, Karmazyn M. NHE-1 inhibition improves impaired mitochondrial permeability transition and respiratory function during postinfarction remodeling in the rat. *J Mol Cell Cardiol* 38: 135–143, 2005.
- Javadov S, Rajapurohitam V, Kilic A, Hunter JC, Zeidan A, Said Faruq N, Escobales N, Karmazyn M. Expression of mitochondrial fusion-fission proteins during post-infarction remodeling: the effect of NHE-1 inhibition. *Basic Res Cardiol* 106: 99–109, 2011.
- Javadov S, Rajapurohitam V, Kilic A, Zeidan A, Choi A, Karmazyn M. Anti-hypertrophic effect of NHE-1 inhibition involves GSK-3beta-

- dependent attenuation of mitochondrial dysfunction. *J Mol Cell Cardiol* 46: 998–1007, 2009.
34. **Karmazyn M.** Amiloride enhances postischemic ventricular recovery: possible role of Na<sup>+</sup>-H<sup>+</sup> exchange. *Am J Physiol Heart Circ Physiol* 255: H608–H615, 1988.
  35. **Karmazyn M.** Mechanisms of protection of the ischemic and reperfused myocardium by sodium-hydrogen exchange inhibition. *J Thromb Thrombolysis* 8: 33–38, 1999.
  36. **Karmazyn M, Gan XT, Humphreys RA, Yoshida H, Kusumoto K.** The myocardial Na<sup>+</sup>-H<sup>+</sup> exchange: structure, regulation, and its role in heart disease. *Circ Res* 85: 777–786, 1999.
  37. **Kusumoto K, Haist JV, Karmazyn M.** Na<sup>+</sup>/H<sup>+</sup> exchange inhibition reduces hypertrophy and heart failure after myocardial infarction in rats. *Am J Physiol Heart Circ Physiol* 280: H738–H745, 2001.
  38. **Le SB, Hailer MK, Buhrow S, Wang Q, Flatten K, Padiaditakis P, Bible KC, Lewis LD, Sausville EA, Pang YP, Ames MM, Lemasters JJ, Holmuhamedov EL, Kaufmann SH.** Inhibition of mitochondrial respiration as a source of adaphostin-induced reactive oxygen species and cytotoxicity. *J Biol Chem* 282: 8860–8872, 2007.
  39. **Lee SH, Kim T, Park ES, Yang S, Jeong D, Choi Y, Rho J.** NHE10, an osteoclast-specific member of the Na<sup>+</sup>/H<sup>+</sup> exchanger family, regulates osteoclast differentiation and survival [corrected]. *Biochem Biophys Res Commun* 369: 320–326, 2008.
  40. **Lifshitz J, Friberg H, Neumar RW, Raghupathi R, Welsh FA, Janmey P, Saatman KE, Wieloch T, Grady MS, McIntosh TK.** Structural and functional damage sustained by mitochondria after traumatic brain injury in the rat: evidence for differentially sensitive populations in the cortex and hippocampus. *J Cereb Blood Flow Metab* 23: 219–231, 2003.
  41. **Mentzer RM Jr, Bartels C, Bolli R, Boyce S, Buckberg GD, Chaitman B, Haverich A, Knight J, Menasche P, Myers ML, Nicolau J, Simoons M, Thulin L, Weisel RD.** Sodium-hydrogen exchange inhibition by cariporide to reduce the risk of ischemic cardiac events in patients undergoing coronary artery bypass grafting: results of the EXPEDITION study. *Ann Thorac Surg* 85: 1261–1270, 2008.
  42. **Mitchell P, Moyle J.** Translocation of some anions and acids in rat liver mitochondria. *Eur J Biochem* 9: 149–155, 1969.
  43. **Murphy E, Allen DG.** Why did the NHE inhibitor clinical trials fail? *J Mol Cell Cardiol* 46: 137–141, 2009.
  44. **Nakamura TY, Iwata Y, Arai Y, Komamura K, Wakabayashi S.** Activation of Na<sup>+</sup>/H<sup>+</sup> exchanger 1 is sufficient to generate Ca<sup>2+</sup> signals that induce cardiac hypertrophy and heart failure. *Circ Res* 103: 891–899, 2008.
  45. **Piot C, Croisille P, Staat P, Thibault H, Rioufol G, Newton N, Elbelghiti R, Cung TT, Bonnefoy E, Angoulvant D, Macia C, Raczka F, Sportouch C, Gahide G, Finet G, Andre-Fouet X, Revel D, Kirkorian G, Monassier JP, Derumeaux G, Ovize M.** Effect of cyclosporine on reperfusion injury in acute myocardial infarction. *N Engl J Med* 359: 473–481, 2008.
  46. **Robin E, Guzy RD, Loor G, Iwase H, Waypa GB, Marks JD, Hoek TL, Schumacker PT.** Oxidant stress during simulated ischemia primes cardiomyocytes for cell death during reperfusion. *J Biol Chem* 282: 19133–19143, 2007.
  47. **Rodriguez-Sinovas A, Cabestrero A, Garcia del Blanco B, Inserte J, Garcia A, Garcia-Dorado D.** Intracoronary acid infusion as an alternative to ischemic postconditioning in pigs. *Basic Res Cardiol* 104: 761–771, 2009.
  48. **Ruiz-Meana M, Garcia-Dorado D, Pina P, Inserte J, Agullo L, Soler-Soler J.** Cariporide preserves mitochondrial proton gradient and delays ATP depletion in cardiomyocytes during ischemic conditions. *Am J Physiol Heart Circ Physiol* 285: H999–H1006, 2003.
  49. **Rupprecht HJ, vom Dahl J, Terres W, Seyfarth KM, Richardt G, Schultheibeta HP, Buerke M, Sheehan FH, Drexler H.** Cardioprotective effects of the Na<sup>+</sup>/H<sup>+</sup> exchange inhibitor cariporide in patients with acute anterior myocardial infarction undergoing direct PTCA. *Circulation* 101: 2902–2908, 2000.
  50. **Sardet C, Franchi A, Pouyssegur J.** Molecular cloning, primary structure, and expression of the human growth factor-activatable Na<sup>+</sup>/H<sup>+</sup> antiporter. *Cell* 56: 271–280, 1989.
  51. **Siemen D, Loupatatzis C, Borecky J, Gulbins E, Lang F.** Ca<sup>2+</sup>-activated K channel of the BK-type in the inner mitochondrial membrane of a human glioma cell line. *Biochem Biophys Res Commun* 257: 549–554, 1999.
  52. **Snabaitis AK, D'Mello R, Dashnyam S, Avkiran M.** A novel role for protein phosphatase 2A in receptor-mediated regulation of the cardiac sarcolemmal Na<sup>+</sup>/H<sup>+</sup> exchanger NHE1. *J Biol Chem* 281: 20252–20262, 2006.
  53. **Szabo I, Bock J, Jekle A, Soddemann M, Adams C, Lang F, Zoratti M, Gulbins E.** A novel potassium channel in lymphocyte mitochondria. *J Biol Chem* 280: 12790–12798, 2005.
  54. **Teshima Y, Akao M, Jones SP, Marban E.** Cariporide (HOE642), a selective Na<sup>+</sup>-H<sup>+</sup> exchange inhibitor, inhibits the mitochondrial death pathway. *Circulation* 108: 2275–2281, 2003.
  55. **Theroux P, Chaitman BR, Danchin N, Erhardt L, Meinertz T, Schroeder JS, Tognoni G, White HD, Willerson JT, Jessel A.** Inhibition of the sodium-hydrogen exchanger with cariporide to prevent myocardial infarction in high-risk ischemic situations. Main results of the GUARDIAN trial Guard during ischemia against necrosis (GUARDIAN) Investigators. *Circulation* 102: 3032–3038, 2000.
  56. **Truscott KN, Brandner K, Pfanner N.** Mechanisms of protein import into mitochondria. *Curr Biol* 13: R326–R337, 2003.
  57. **Wang Y, Meyer JW, Ashraf M, Shull GE.** Mice with a null mutation in the NHE1 Na<sup>+</sup>-H<sup>+</sup> exchanger are resistant to cardiac ischemia-reperfusion injury. *Circ Res* 93: 776–782, 2003.
  58. **Xue J, Mraiche F, Zhou D, Karmazyn M, Oka T, Fliegel L, Haddad GG.** Elevated myocardial Na<sup>+</sup>/H<sup>+</sup> exchanger isoform 1 activity elicits gene expression that leads to cardiac hypertrophy. *Physiol Genomics* 42: 374–383, 2010.
  59. **Zeymer U, Suryapranata H, Monassier JP, Opolski G, Davies J, Rasmanis G, Linssen G, Tebbe U, Schroder R, Tiemann R, Machnig T, Neuhaus KL.** The Na<sup>+</sup>/H<sup>+</sup> exchange inhibitor eniporide as an adjunct to early reperfusion therapy for acute myocardial infarction. Results of the evaluation of the safety and cardioprotective effects of eniporide in acute myocardial infarction (ESCAMI) trial. *J Am Coll Cardiol* 38: 1644–1650, 2001.

**A****B**

**Supplemental Figure 1. Swelling of rat heart mitochondria induced by CaCl<sub>2</sub>**

**A**, Sample scattered light absorbance trace in the absence of CaCl<sub>2</sub>, for heart mitochondria isolated from rats transduced with shRNA-SCR (SCR, scramble, control). **B**, Summary results of % of light scattering decrease in rats transduced with shRNA-SCR, or rats transduced with shRNA-NHE1, before and after treatment with Cyclosporine 1 μM. \*P<0.05 vs. SCR (ANOVA).